Progress in Oceanography 219 (2023) 103132

Contents lists available at ScienceDirect

Progress in Oceanography

journal homepage: www.elsevier.com/locate/pocean

Seasonal patterns of vertical flux in the northwestern Barents Sea under Atlantic Water influence and sea-ice decline

Yasemin V. Bodur [a,*], Paul E. Renaud [b], Lucie Goraguer [c], Martí Amargant-Arumí [a], Philipp Assmy [c], Anna Maria Dąbrowska [d], Miriam Marquardt [a], Angelika H.H. Renner [e], Agnieszka Tatarek [d], Marit Reigstad [a]

[a] UiT – the Arctic University of Norway, Tromsø, Norway
[b] Akvaplan-niva, Tromsø, Norway
[c] Norwegian Polar Institute, Tromsø, Norway
[d] Institute of Oceanology Polish Academy of Science (IOPAN), Poland
[e] Institute of Marine Research, Tromsø, Norway

ARTICLE INFO

Keywords:
Carbon export
Polar Front
Marginal ice zone (MIZ)
Seasonal ice zone (SIZ)
Seasonality
Attenuation

ABSTRACT

The northern Barents Sea is a productive Arctic inflow shelf with a seasonal ice cover and as such, a location with an efficient downward export of particulate organic matter through the biological carbon pump. The region is under strong influence of Atlantification and sea-ice decline, resulting in a longer open water and summer period. In order to understand how these processes influence the biological carbon pump, it is important to identify the seasonal and spatial dynamics of downward vertical flux of particulate organic matter. In 2019 and 2021, short-term sediment traps were deployed between 30 and 200 m depth along a latitudinal transect in the northwestern Barents Sea during March, May, August and December. Vertical flux of particulate organic carbon, $\delta^{13}C$ and $\delta^{15}N$ values, Chl-*a*, protists and fecal pellets were assessed. We identified a clear seasonal pattern, with highest vertical flux in May and August (178 ± 202 and 159 ± 79 mg C m^{-2} d^{-1}, respectively). Fluxes in December and March were < 45 mg C m^{-2} d^{-1}. May was characterized by diatom- and Chl *a*-rich fluxes and high spatial variability, while fluxes in August had a higher contribution of fecal pellets and small flagellates, and were spatially more homogenous. Standing stocks of suspended particulate organic matter were highest in August, suggesting a more efficient retention system in late summer. The strong latitudinal sea-ice gradient and the influence of Atlantic Water probably led to the high spatial variability of vertical flux in spring, due to their influence on primary productivity. We conclude that the efficiency of the biological carbon pump in a prolonged open-water period depends on the reworking of small, slow sinking material into efficiently sinking fecal pellets or aggregates, and the occurrence of mixing.

1. Introduction

The Barents Sea is the largest inflow shelf of the Arctic Ocean, and with an annual primary production of 20–200 g C m^{-2} yr^{-1} it is also one of the most productive Arctic shelf seas (Wassmann et al., 2006; Sakshaug et al., 2009). Over the last decades, the northern Barents Sea has experienced the largest sea ice loss across the Arctic Ocean (Screen and Simmonds, 2010; Onarheim et al., 2018; Smedsrud et al., 2022). Moreover, the heat and inflow of warm (>2 °C) and saline (>35.06 g kg^{-1}) Atlantic Water (AW) in this region is increasing (Oziel et al., 2020; Polyakov et al., 2020; Skagseth et al., 2020; Ingvaldsen et al., 2021; Smedsrud et al., 2022; AW definition following Sundfjord et al., 2020). This "Atlantification" is predicted to have significant consequences for the marine ecosystem in this region and thus, for the cycling and export of organic carbon (Wassmann and Reigstad, 2011).

Over the last century, the uptake of atmospheric CO_2 by the Arctic Ocean has increased by around 30% (Smedsrud et al., 2022). An especially tight pelagic-benthic coupling has been documented in the marginal sea-ice zone (MIZ) in the northern Barents Sea (Wassmann et al., 2006). Thus, the biological carbon pump in the Barents Sea is an important sink for anthropogenic carbon as well as a crucial food source for benthic communities in the region (Carroll et al., 2008). It is therefore important to

* Corresponding author.
E-mail address: yasemin.bodur@uit.no (Y.V. Bodur).

https://doi.org/10.1016/j.pocean.2023.103132

Available online 27 September 2023

investigate the strength of the biological carbon pump across the marginal or seasonal ice zone today, in order to evaluate potential responses to future climate change.

As a consequence of earlier ice melt and later onset of freezing, earlier phytoplankton blooms and a longer productive period in the MIZ are predicted (Ellingsen et al., 2008; Slagstad et al., 2015; Polyakov et al., 2020), resulting in longer summer conditions (Wassmann and Reigstad, 2011). While remote sensing from satellites have shown an increase of annual primary production in the northern Barents Sea (Arrigo and van Dijken 2015; Dalpadado et al. 2014; Lewis et al. 2020), the stratification regime and nutrient availability will most likely determine whether there will be an increase or a decrease in a future warmer central and southern Barents Sea (Slagstad et al., 2011; Mousing et al., 2023).

The efficiency of the biological carbon pump depends not only on primary production, but on a number of regulating mechanisms, such as grazing and fecal pellet production by zooplankton, aggregation and disaggregation of particles, microbial processes, ballasting by minerals, vertical mixing and stratification of the upper water column (De La Rocha and Passow, 2007; Turner, 2015; Iversen, 2023). Since retention processes dominate in the pelagic realm, vertical flux is typically "attenuated" sharply in surface waters, and usually less than 10% of primary production reaches below the mesopelagic zone (Martin et al., 1987; Wassmann et al., 2003). Highest export has most often been measured during peak bloom events in spring (Reigstad et al., 2008; Dybwad et al., 2021). While nutrients decrease as the season proceeds, the carbon flux is increasingly dominated by regenerated material orginating from blooms of lower magnitude with a higher fraction of small cells during summer (late bloom scenarios; Reigstad et al., 2008; Dybwad et al., 2021; Trudnowska et al., 2021). Small cells usually sink less efficiently and are more often coupled to a tight microbial food web, leading to higher retention in the surface water column (Wassmann et al., 2006) and a reduced efficiency of the biological carbon pump. Thus, a prolonged summer season and increased light availability for primary production will not necessarily result in higher export of carbon (Wassmann and Reigstad, 2011). However, if a sufficiently high amount of small and reworked particles is present and vertical flux attenuation is weak, these particles can contribute significantly to vertical flux (Wiedmann et al., 2014).

As an Arctic inflow shelf, the northern Barents Sea is under strong influence of AW, which impacts physical and biological properties in the region such as amplified warming, reduced sea ice thickness, enhanced upper ocean mixing, nutrient supply, advection of organic material and increased primary production (Polyakov et al., 2020; Skagseth et al., 2020; Ingvaldsen et al., 2021). Another consequence is that boreal zooplankton are expanding northwards in the Barents Sea (Ellingsen et al., 2008; Drinkwater, 2011; Dalpadado et al., 2012; Fossheim et al., 2015; Eriksen et al., 2017), altering pelagic communities and their functions (Renaud et al., 2018). These changing properties are termed "Atlantification". Increased metabolic activity due to warming (Wohlers et al., 2009) and an increase of grazers could lead to enhanced degradation of organic matter in the water column. On the other hand, grazers can enhance vertical flux by packaging the production into fast-sinking fecal pellets (Wexels Riser et al., 2008), which can substantially contribute to vertical flux in the Barents Sea (Wiedmann et al., 2014; Dybwad et al., 2022).

Only a few studies have been carried out in the Arctic Ocean that integrate the effects of temporal (seasonal), spatial and depth gradients of vertical flux and its composition (e.g. Olli et al., 2002; Reigstad et al., 2008; Dybwad et al., 2021), and we are aware of only 3 studies that deployed short-term sediment traps at revisited stations (Lalande et al., 2016a; Walker et al., 2022; Wiedmann et al., 2016). However, these are from Arctic fjords and do not integrate spatial variability. In order to fill this gap for the seasonally ice-covered northern Barents Sea, we revisited stations along a latitudinal transect in 2019 and 2021 during different seasons reflecting potential changes in drivers most strongly impacted by climate change (sea ice, water masses). Short-term sediment traps were deployed to assess daily vertical flux patterns and its composition. We attempted to 1. describe seasonal and spatial patterns in vertical flux, 2. identify the importance of environmental (sea ice, water mass) and biological drivers contributing to the observed patterns and 3. explore the implications of these results in a changing Arctic Ocean.

2. Methods

2.1. Study area and short-term sediment trap deployment

The study was carried out within the framework of the Norwegian research project The Nansen Legacy. Fieldwork took place in August and December 2019, and March and May 2021 at 6 stations following a transect between 75° and 85°N along the 30°E meridian in the northern Barents Sea (Fig. 1) aboard the Norwegian icebreaker *RV Kronprins Haakon*.

Stations P1, P2, P4, and P5 were on the shelf whereas P6 was on the northern Barents Sea slope and P7 was in the Nansen Basin (Fig. 1). The northern Barents Sea shelf is around 300 m deep, while two stations on the shelf (P2 and P5) were located on shallower banks and are <200 m deep. The positions of stations P6 and P7 varied somewhat due to ice conditions during the different cruises. Thus, the depth at station P6 varied between ~800–1500 m while station P7 in the Nansen Basin had a water depth of >3000 m (Table 1).

Atlantic Water (AW) enters the central and northern Barents Sea via two pathways (Fig. 1). One pathway is through the Barents Sea Opening between mainland Norway and Bjørnøya towards the southern Barents Sea, where P1 is situated, and continuing eastwards (Ingvaldsen et al., 2002; Ingvaldsen et al., 2004). The second pathway follows the continental slope first west then north of Svalbard (Beszczynska-Möller et al. 2012). From there, AW enters the northern Barents Sea through two troughs on either side of Kvitøya (Lind and Ingvaldsen, 2012; Lundesgaard et al., 2022).

During the sampling campaigns, station P1 was influenced by warm and saline AW or modified AW (mAW: AW that has lost heat; Sundfjord et al., 2020) throughout the water column. In August, P1 displayed presence of warm (<0ºC) Polar Water at the surface (wPW; Sundfjord et al. 2020). wPW is usually PW that is warmed by AW from below, or by solar radiation at the surface. Stations P2, P4 and P5 were mainly characterized by Polar Water (PW), with wPW dominating below 100 m during March and above 40 m during August. During March and May, stations P6 and P7 were dominated by wPW below ~ 50 m, while PW dominated at the surface. In August and December, a deep core of AW was present below 100 m at these stations.

Short-term drifting sediment traps (KC Denmark, aspect ratio > 6) were deployed during each sampling campaign at 6 depths (30, 40, 60, 90, 120 and 200 m) for a duration between 18 and 38 h, with longer deployment times during periods of low vertical flux. At stations shallower than 250 m, the deepest trap was at 120 m. In order to ensure settling of particles into the traps, the cylinders were filled with prefiltered (0.7 μm GF/F Whatman) high-density bottom water. The traps were deployed without poison in open water, sea ice leads or anchored to a sea ice floe, depending on the sea ice conditions at the station.

2.2. Subsampling for biogeochemical and biological analysis

After sediment trap retrieval, the content of all traps (2 or 4 cylinders) at each depth were pooled and kept cold and dark until subsamples were taken for size fractionated chlorophyll *a* (Chl-*a;* Bodur et al. 2023a–d), fecal pellets (FP; Bodur et al. 2023e–h), protist community composition (Bodur et al. 2023i–l), particulate organic carbon and particulate nitrogen (POC and PN; Bodur et al. 2023m–p), and stable isotopes (SI; Bodur et al. 2023q–t).

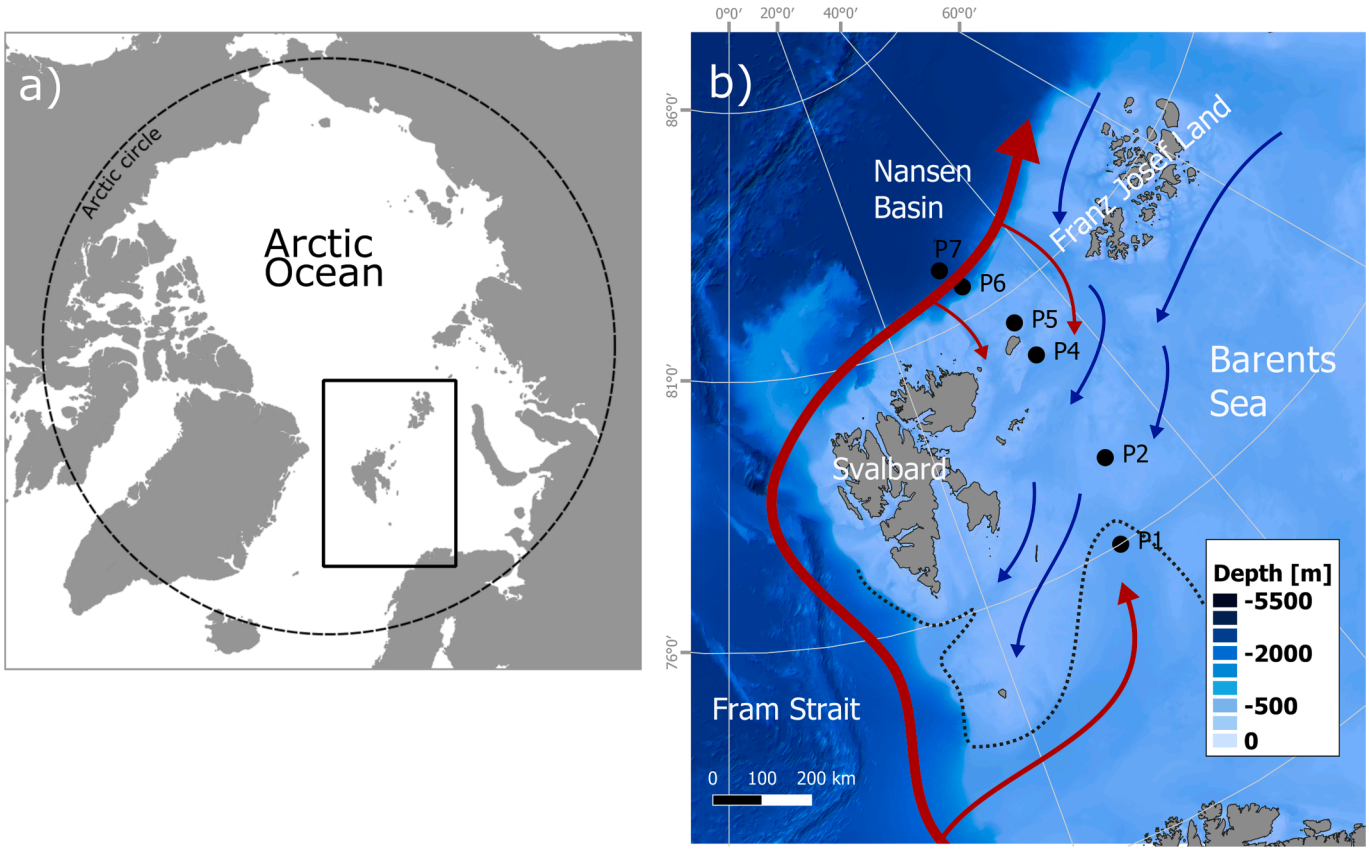

Fig. 1. Map of the a) Arctic Ocean, showing the study area in the black rectangle, and b) nominal sampling locations in the central and northwestern Barents Sea during August 2019, December 2019, March 2021 and May 2021, general patterns of inflowing Atlantic Water along and onto the shelf (red arrows), general patterns of surface Polar Water (blue arrows) and approximate location of the Polar Front (dashed line, after Onarheim and Teigen 2018). For actual sampling locations during each individual cruise see Table 1. Bathymetry obtained from the International Bathymetric Chart of the Arctic Ocean (IBCAO; Jakobsson et al., 2020) and coastlines from Wessel & Smith (1996), plotted with QGIS 3.28.2.

Table 1
Sampling locations and details for short-term sediment trap deployments during August and December 2019 and March and May 2021 in the northwestern Barents Sea. Daily sea ice concentration data for station locations were retrieved from Steer and Divine (2023) and mean % ice cover is calculated from the 4 weeks preceding the respective sampling date. Chl-*a* data was retrieved from Vader (2022a–d), and the depth of Chl-*a* maximum is shown within paranthesis.

Station	Latitude	Longitude	Deployment date	Depth (m)	Deployment duration (hours)	Mean % ice cover	Max susp. Chl *a* (mg m^{-3})
P1	76.00	31.22	08.08.2019	325	23.55	0 ± 0	1.22 (55 m)
P4	79.78	33.97	13.08.2019	330	19.10	8 ± 17	1.37 (30 m)
P5	80.50	33.88	15.08.2019	157	20.67	92 ± 8	2.57 (20 m)
P6	81.57	31.22	18.08.2019	861	18.15	96 ± 4	1.29 (10 m)
P7	81.93	29.16	21.08.2019	3312	24.75	96 ± 5	1.74 (10 m)
P4	79.82	34.17	08.12.2019	271	27.77	100 ± 1	0.02 (121 m)
P7 (DEEP-ICE)	82.06	29.22	01.12.2019	3433	41.75	98 ± 2	0.04 (20 m)
P4	79.74	33.88	09.03.2021	334	38.72	97 ± 3	N.A.[a]
P5	80.52	33.99	12.03.2021	162	25.80	85 ± 20	0.01 (30 m)
P6	81.54	31.02	14.03.2021	789	27.13	28 ± 34	0.02 (10 m)
P7	82.00	29.98	16.03.2021	3299	33.53	20 ± 35	0.02 (10 m)
P1	76.00	31.22	01.05.2021	326	11.97	0 ± 0	1.66 (50 m)
P2	77.50	33.96	02.05.2021	188	11.68	21 ± 31	1.29 (50 m)
P4	79.75	33.97	04.05.2021	359	26.75	71 ± 33	2.13 (50 m)
P5	80.50	34.07	07.05.2021	162	25.85	96 ± 4	0.69 (10 m)
P6	81.56	30.76	09.05.2021	1557	23.3	92 ± 7	3.17 (30 m)
P7	82.12	29.13	13.05.2021	3369	26.12	96 ± 4	0.29 (90 m)

[a] Not available.

Subsamples for Chl-*a* were filtered in triplicates onto GF/F (Whatman, 0.7 μm) filters and filtered volumes ranged from 100 to 300 ml depending on the amount of material in the traps. Additional samples for Chl-*a* were filtered on 10 μm polycarbonate filters (Millipore) to quantify the contribution from larger cells.

Triplicates of 250–1000 ml were filtered for POC/PN and SI, respectively, onto pre-combusted GF/F filters. POC samples were stored at −20 °C and SI samples at −80 °C until further processing.

250 ml from each depth was fixed with hexamethylenetetramine-buffered 37% formaldehyde (final pH = 7) to a final concentration of

4% for microscopic inspection of fecal pellets, and 100 ml was fixed with a mixture of glutaraldehyde-lugol for protist examination (Rousseau et al., 1990).

2.3. Biogeochemical analysis

Size-fractionated Chl-*a* (0.7 and 10 μm) was extracted from the filters in 100% methanol at 4 °C after filtration and measured on board within 12–24 h after sampling (modified after Holm-Hansen and Riemann, 1978) with a pre-calibrated Turner Design AU-10 fluorometer in 2019 and Turner Triology in 2021 before and after acidification with 5% HCl. Concentrations of Chl-*a* pigments and their phaeopigment degradation products were calculated according to Holm-Hansen and Riemann (1978).

Filters for POC and PN were dried for 24 h at 60° C and subsequently acid fumed (HCl) for 24 h in order to remove all inorganic carbon. Afterwards, the samples were again dried for 24 h at 60° C, transferred to tin capsules and measured with an Exeter Analytical CE440 CHN elemental analyzer.

Standards for isotopic ratios for carbon and nitrogen were Vienna PeeDee belemnite and air, respectively. Alanine (JALA, Fischer Scientific) was used for internal quality assurance with an analytical precision of $\delta^{13}C_{VPDB}$ = -20.59 ± 0.05 ‰ (n = 47 runs) and $\delta^{15}N_{AIR}$ = -3.16 ± 0.10 ‰ (n = 57 runs), respectively. L-glutamic acid (JGLUT, Fischer Scientific) and glycine (POPPGLY, Fischer Scientific) were used as internal reference material. Internal references and quality assurance for $\delta^{13}C_{VPDB}$ were calibrated against calcium carbonate (NBS19) and lithium carbonate (LSVEC) with consensus values 1.95 ‰ and −46.6 ‰, respectively, and for $\delta^{15}N_{AIR}$ against L-glutamic acid (USGS40 and USGS41) with consensus values −4.52 ‰ and 47.57 ‰, respectively.

2.4. Analysis of vertical flux particle composition

Protists, including phyto- and protozooplankton, were identified to the lowest possible taxonomic level in accordance with the World Register of Marine Species (WoRMS) and counted under an inverted light microscope (Nikon Eclipse TE-300 and Ti-S) using the Utermöhl method (Utermöhl, 1958; Edler and Elbrächter, 2010). Between 23 and 2301 cells (December and May, respectively) were counted per sample (mean: 531 ± 595 cells per sample across all sample dates and stations). Abundances were converted to carbon biomass based on published geometric relationships for biovolume conversion (Hillebrand et al., 1999) and biovolume to carbon conversion factors (Menden-Deuer and Lessard, 2000). Radiolaria (12 recorded instances with < 4 individuals counted) and Foraminifera (1 instance with 1 count) were kept in the community composition data, but were removed from biomass estimations as no size measurements were available and thus carbon estimates could not be made for these groups.

Depending on their density in the sample, subsamples of 25–100 ml were taken for fecal pellet analysis and settled in Utermöhl sedimentation chambers for 24 h. Subsequently they were counted and the length and width of each fecal pellet were measured using a Leica inverted microscope. The condition of each pellet was noted (intact, end piece or mid piece). Long and cylindrical pellets were attributed to calanoid copepods, small ellipsoid pellets to appendicularians, and larger strings with cut ends to euphausiids (Dybwad et al. 2021). Larger and irregularly shaped ellipsoid pellets were attributed to chaetognaths (Dilling and Alldredge 1993; Giesecke et al. 2010). Micropellets were ignored because they can be difficult to distinguish from protozoans or detritus.

Based on the pellet types, the volume for each pellet was calculated and their carbon content was assessed using empirical conversion factors of 94.3 μg C mm^{-3} for copepod, 45.1 μg C mm^{-3} for krill and 25.1 μg C mm^{-3} for appendicularian pellets after Wexels Riser et al. (2007), 12.73 μg C mm^{-3} for chaetognath pellets after Giesecke et al. (2010) and 69.4 μg C mm^{-3} for unidentified pellets after Riebesell et al. (1995).

The percentage contribution of fecal pellet carbon (FPC) and protist carbon (PC) to total POC are estimates using empirically determined conversion factors, largely from other locations and seasons as stated above. This sometimes resulted in higher FPC or PC estimations than total measured POC. Manno et al. (2015) showed that FPC content can be lower in late autumn/winter in the Southern Ocean and Franco-Santos et al. (2018) demonstrated different FPC content under contrasting nutrient conditions; however, Urban-Rich (1997) showed that there was no difference in carbon to volume ratio between food types and different locations.

2.5. Statistical analyses

All statistical analyses were performed in the computing software R (version 4.2.2), using the vegan package (Oksanen et al., 2018). An unconstrained correspondence analysis (CA) was performed on log-transformed protist community data in order to downweigh stations with high abundances. A second CA was run on biomass data. In order to delineate which groups (diatoms, dinoflagellates, ciliates, *Phaeocystis*, other flagellates) dominated the vertical flux at the respective stations during each season, they were plotted on top of the ordination. To understand how POC fluxes were related to the protist community composition, they were displayed by isolines.

In order to describe how bulk flux characteristics differed at each station during each season, a principal component analysis (PCA) on scaled (centered to mean of zero) flux variables (POC, POC:PN ratio, FPC, PC, protist abundance, Chl-*a*, % of Chl-*a* > 10 μm, Chl-*a*:Phaeopigment ratio) was performed. Subsequently, environmental (sea ice, salinity, temperature and water mass) and suspended biological (integrated suspended POC, POC:PN ratio, Chl-*a*, Chl-*a*:Phaeogiment ratio, % of Chl-*a* > 10 μm, integrated protist abundance and biomass) parameters were fitted on top of the ordination in order to visualize how they may be related to the vertical flux patterns. The fitted data were standardized prior to analysis.

Environmental and biological parameters were retrieved for all seasonal cruises from the following sources: CTD data for salinity and temperature, from Gerland (2022); Ludvigsen (2022); Reigstad (2022) and Søreide (2022); water masses were assigned according to Sundfjord et al. (2020); suspended POC data were obtained from Marquardt et al. (2022a–d); suspended Chl-*a* data, from Vader (2022a–d); and suspended protist diversity, from Assmy et al. (2022a–d). Sea ice concentration data for station locations were retrieved from Steer and Divine (2023), which uses AMSR-2 and AMSR-E sea ice concentration products, and the mean sea ice concentration from one month prior to sampling at the respective station was computed and used for the PCA analysis.

3. Results

3.1. Seasonal and spatial patterns of sinking particulate organic matter

In May and August, vertical flux of POC averaged across all stations was similar, but the variability among stations was higher in May than in August (178 ± 199 and 159 ± 97 mg C m^{-2} d^{-1}, respectively; Fig. 2). By contrast, mean chlorophyll *a* (Chl-*a*) fluxes differed substantially between seasons (Fig. 3), with highest vertical flux in May (mean 8 ± 11 mg Chl-*a* m^{-2} d^{-1}), followed by August (mean 1 ± 0.4 mg Chl-*a* m^{-2} d^{-1}).

Highest POC fluxes were measured during May at P1 with no attenuation (604 ± 18 mg C m^{-2} d^{-1} across all depths) and at P6 with high POC fluxes at 30 m (416 mg C m^{-2} d^{-1}) that attenuated by 50% at 60 m. At all other stations, POC fluxes were much lower and did not change much with depth (68 ± 28 mg C m^{-2} d^{-1} across all stations and depths). Similar to the patterns in POC, Chl-*a* fluxes were highest during May at P1, with very high values of 32 ± 1 mg Chl-*a* m^{-2} d^{-1} across all depths, and at 30 m at P6 (25 mg Chl-*a* m^{-2} d^{-1}), while they were much lower at all other stations and depths (1.8 ± 1.4 mg Chl-*a* m^{-2} d^{-1}).

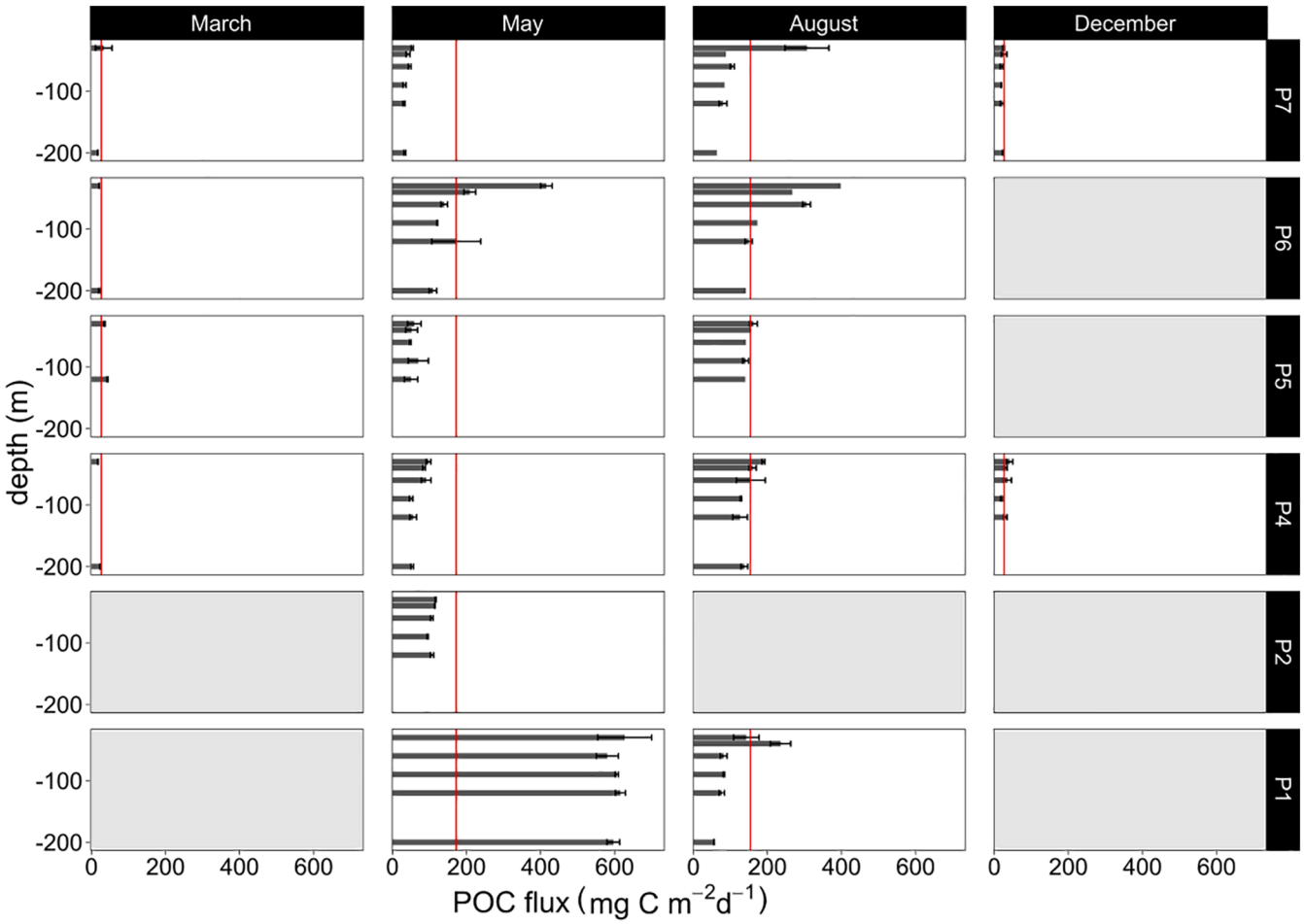

Fig. 2. Mean vertical POC fluxes and standard deviations of three replicate sub-samples across all seasons and stations in the northwestern Barents Sea. Red vertical lines depict the mean vertical flux across all depths and stations for the respective season. Stations are presented according to their position along the latitudinal gradient from south (P1) to north (P7).

In August, highest vertical POC fluxes were observed at 30 m at the northernmost stations, P6 and P7 (531 and 307 mg m^{-2} d^{-1}), but at both stations, fluxes were attenuated quickly by 50% and 30% at 40 m, respectively. At all other stations, there was little attenuation, and average fluxes were 137 ± 44 mg C m^{-2} d^{-1} across all stations and depths. Chl-*a* fluxes ranged between 0.1 at P1 and 1.7 mg Chl-*a* m^{-2} d^{-1} at P6.

In December and March, average POC flux across all stations and depths was 27 ± 7 and 27 ± 9 mg C m^{-2} d^{-1}, respectively. Chl-*a* fluxes during both months were < 0.03 mg Chl-*a* m^{-2} d^{-1}. During March, at the shelf stations (P4, P5) and on the shelf break (P6) POC and Chl-*a* fluxes at 120 or 200 m were slightly elevated. POC fluxes were 1–8 mg C m^{-2} d^{-1} higher relative to 30 m.

In May, POM was most depleted in ^{15}N, with a mean δ^{15}N value of +3.09 ± 1.15 ‰, indicating fresher OM (Fig. 4). Over the course of the season (May, August, December, March) POM became more and more enriched in ^{15}N, until highest values of δ^{15}N were present in March (mean of +8.92 ± 0.57 ‰ across all stations). A high variation among stations in May is visible along the δ^{13}C axis, with lowest δ^{13}C values at P2 (−28.89 ‰) and P7 (−28.29 ‰) and highest values at P1 and P6 (~−21 ‰). With progressing season, values for all stations converge along the δ^{13}C axis. While in August the range in δ^{13}C values among stations was already lower (between −27.28 ‰ at P4 and −21.95 ‰ at P6), in December, δ^{13}C among all stations varied only between −26.42 ‰ and –23.59 ‰. In March, δ^{13}C values were between –23.80 and −25.72 ‰ at P7 at 30 m. At all the other stations, however, samples more enriched in ^{13}C were measured at the 120 and 200 m traps at P4, P5 and P6 (−21.77 to −21.38 ‰).

3.2. Composition and drivers of vertical flux

For May and August, carbon conversions applied to fecal pellets and protists occasionally led to overestimates of the contribution of protist carbon (PC) and fecal pellet carbon (FPC) to total POC, resulting in estimates > 100% of total POC. The contribution of PC to total POC was highly variable during May and August across the transect, with 2 – 98% in May across all stations and depths, 8 – 100% in August, <15% in December and < 3% in March. (Fig. 5). Fecal pellet carbon made up a significant fraction of total POC flux during May and August, particularly at P4, P5, and P6 where it contributed up to 100%, while at the other stations it usually contributed < 30%. In both March and December, there were few recognizable cells or fecal pellets, resulting in a higher amount of detritus contributing to bulk POC (>94% in March and > 65% in December). In March, there was a slightly higher number of recognizable cells at depth compared to the surface. In December, up to 5 mg C m^{-2} d^{-1} (10–25% total POC flux) could be attributed to PC, mostly from ciliates.

During degradation of organic matter, N is remineralised faster than C, resulting in increased POC:PN ratios of more degraded material. Ratios were highest in winter (6 – 10 in March and 8 – 11 in December) and lowest in spring (5 – 7 across all stations and depth; except for at P7 where ratios were very high, ranging between 8 and 11 across all depths;

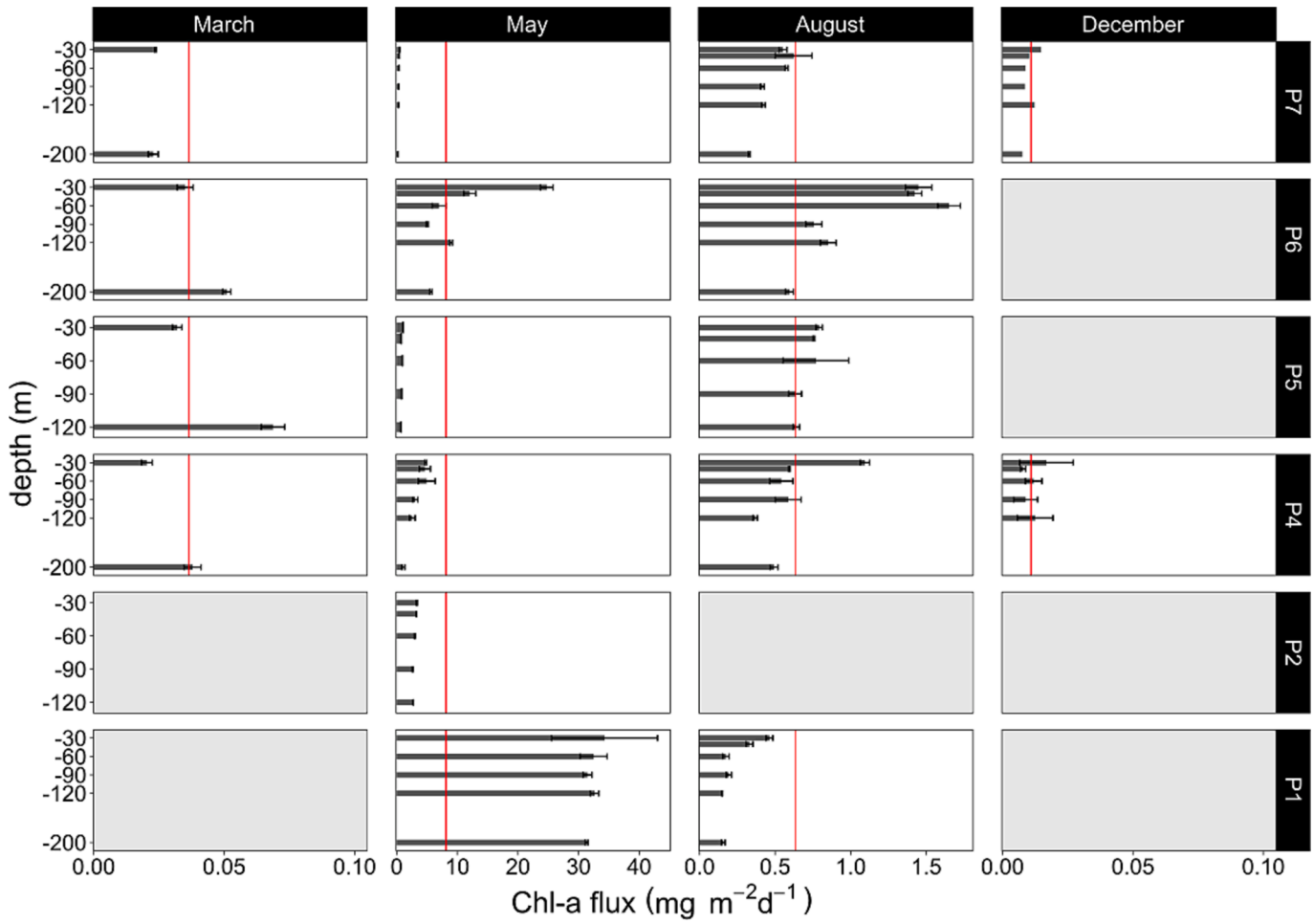

Fig. 3. Mean vertical Chl-*a* fluxes and standard deviations of three replicate sub-samples across all seasons and stations in the northwestern Barents Sea. Red vertical lines depict the mean vertical flux across all depths and stations for the respective season. Stations are presented according to their position along the latitudinal gradient from south (P1) to north (P7). Note the different scales on the x-axes.

Fig. 6). POC:PN ratios usually increased with depth across all seasons and stations, except for in March at stations P4 and P6. Chl-*a*:Phaeo ratios reflect the freshness of algal material since phaeopigments are a degradation product of Chl-*a*. The Chl-*a*:Phaeo ratios were highest in May, ranging between 1.3 (P4) – 4.8 (P1), also showing high variability among stations. In August, ratios ranged between 0.5 and 2.3 and decreased with depth, while in March they were between 0.1 and 2. In December, Chl-*a*:Phaeo ratios were lowest, with < 0.003 across all stations. Chl-*a*:POC ratios reflects the contribution of photosynthetic algae to the organic matter pool. They were low in March, August and December, with ratios < 0.007. In contrast, in May they varied between 0.006 at P7 to 0.06 at P4. The percentage of total Chl-*a* found in cells larger than 10 μm (% Chl-*a* > 10 μm) was generally higher in May than in August (69% ± 0.3 and 49% ± 0.2, respectively; Figure S1).

To identify key drivers and similarities of the protist community contributing to the vertical flux, two correspondence analyses (CA) were performed on protist cell and biomass fluxes, respectively. The patterns of the two CAs were very similar and therefore the results are not shown for biomass fluxes. All fitted protist groups were significantly correlated with the ordination ($p < 0.003$). The two first axes of the CA explained a low, but similar amount of the total variance (8.8 and 6.2%, respectively; Fig. 7, Table S1) and indicated a clear seasonal gradient in their combination.

In anti-clockwise direction, stations in May, which were mostly aligned along the second CA axis, were followed by stations in August that correlated negatively with the first CA axis, then followed by stations in December and finally stations March, which were both negatively correlated with the second CA axis. This lead to a separation of all stations by productivity along the second CA axis, with August and productive May stations positively correlated with the axis, and the winter (December and March) and less productive May stations negatively correlated. Along the first axis, stations were separated by the different protist groups, with May stations strongly driven by diatoms, while in August they were driven by *Phaeocystis*, ciliates, dinoflagellates and other flagellates.

The gradient in POC flux clearly increased with high diatom abundances in May (isolines; Fig. 7), whereas the winter communities indicated lower POC fluxes across stations. This clear gradient was also reflected in Chl-*a* flux (not shown).

A PCA biplot of the measured vertical flux parameters is shown in Fig. 8a and identifies seasonal characteristics of the vertical flux. Along the first axis (explaining 44.7% of the total variance among samples), stations are clearly separated by vertical flux gradients: May and August grouped on the right-hand side, strongly driven by high POC fluxes, while the winter fluxes are grouped further to the left on this axis, driven by high POC:PN ratios. Along the second axis (explaining 20.1% of the variance), fluxes in August are separated from May. While vertical flux in August was strongly driven by high protist abundance, protist biomass and fecal pellet carbon, vertical flux in May was driven by fresher material, indicated by high Chl-*a*, mainly large cells (defined by % Chl-*a* > 10 μm), and high Chl-*a*:Phaeopigments ratios.

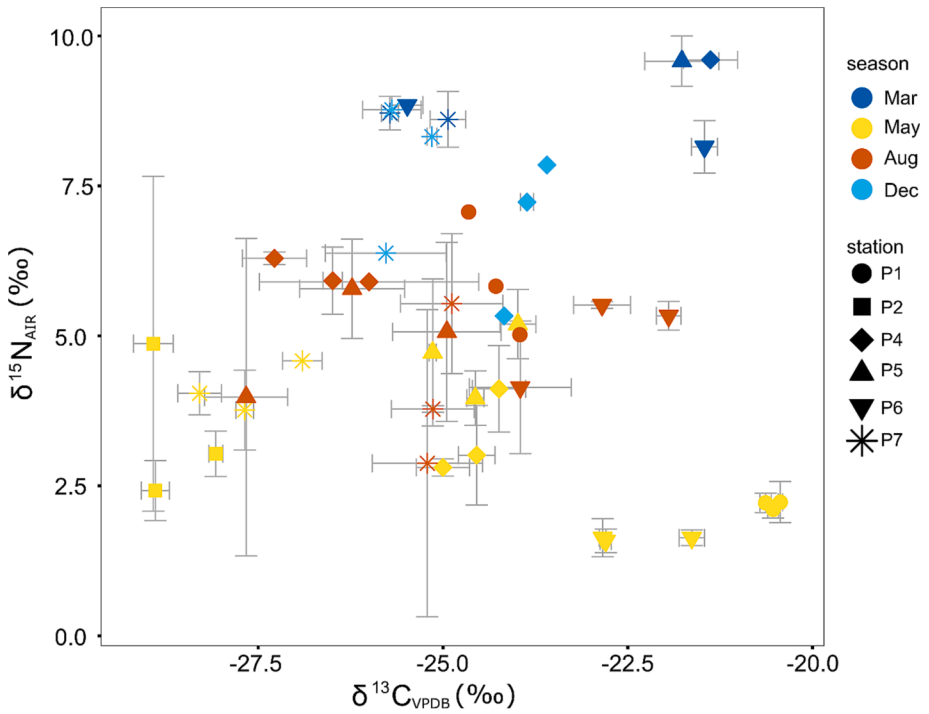

Fig. 4. $\delta^{13}C_{VPDB}$ and $\delta^{15}N_{AIR}$ values for sediment trap particulate organic matter across all seasons and stations in the northern Barents Sea. Seasons are distinguished by color and stations by symbols. Standard deviations are depicted by grey errorbars and are based on 2-3 replicates.

When environmental (sea ice, salinity, temperature and water mass) and biological parameters (integrated suspended POC, POC:PN ratio, Chl-*a*, Chl-*a*:Phaeogiment ratio, % of Chl-*a* > 10 μm, integrated protist abundance and biomass) are fitted on top of this ordination, AW is associated with vertical flux in August, while modified AW (mAW) is associated with vertical flux in May. Integrated suspended Chl-*a* correlates with the fluxes in May, while suspended POC correlates with fluxes in August. Along the first axis, temperature and suspended integrated Chl-*a* (Fig. 8b) as well as Chl-*a* flux (Fig. 8a) are pointing in the same directions, while along the second axis total suspended POC and % of Chl-*a* > 10 μm are pointing into opposite directions. High suspended POC:PN ratios are correlated with the vertical flux in winter. All fitted variables except for POC:PN, protist abundance and protist biomass were significantly correlated to the ordination ($p < 0.02$).

4. Discussion

Vertical flux of particulate organic matter measured in the northwestern Barents Sea in August and December 2019 and March and May 2021 displayed strong seasonal differences in vertical flux magnitude with highest values during the productive season from early spring to summer. Moreover, we identified conspicuous differences in the composition and quality of vertical flux between spring (May) and summer (August). Interestingly, during May we did not observe a strictly latitudinal gradient of vertical flux patterns following the northwards retreat of the sea ice edge. Instead, we measured high vertical flux under pack-ice at one of the northernmost regions, possibly influenced by the warm Atlantic Water flowing eastwards along the Barents Sea shelf break.

4.1. Characterizing spring and summer during heterogenous conditions in the seasonally ice-covered northern Barents Sea

The identified strong seasonal pattern is consistent with previous seasonal vertical flux measurements conducted with short-term sediment traps in the same region (Andreassen and Wassmann, 1998; Olli et al., 2002), and other regions in the Arctic (Dezutter et al., 2021; Dybwad et al., 2021; Fadeev et al., 2021; Koch et al., 2020; Lalande et al., 2016a,b; Nöthig et al., 2015). Highest POC fluxes were measured in May and August (Fig. 2), moving from a fresh, diatom-derived flux in spring (May) to a vertical flux dominated by small and increasingly heterotrophic cells in summer (August), especially by *Phaeocystis* (Figs. 7, 8 and S2). In August, Chl-*a* fluxes, Chl-*a*:POC and Chl-*a*:Phaeo ratios were lower than in May (Fig. 7), indicating reduced algal biomass and freshness of the sinking OM during summer. In winter (December and March), vertical flux was negligible (Fig. 2) and was mostly comprised of unidentifiable detritus (Fig. 5), suggesting low export from a heterotrophic pelagic system dominated by ciliates and heterotrophic flagellates.

This seasonal pattern was also reflected in the increasingly positive $\delta^{15}N$ values of sinking organic matter (OM) with progressing season from spring to winter, where each sampling period was clearly separated along the $\delta^{15}N$ axis (Fig. 4). When nitrate is abundant, algal cells preferentially take up the lighter ^{14}N isotope, which leads to POM being depleted in ^{15}N (Peterson and Fry 1987; Tamelander et al. 2009). Accordingly, we measured the lowest $\delta^{15}N$ values across the whole transect during spring (May), when nutrients were abundant and the increasing incident light started to allow for primary production (Figure S3). With progressing season, nutrients became increasingly reduced, which led to an intensified uptake of the heavier isotope, and increasingly regenerated and degraded material in the water column towards winter further led to OM enriched in ^{15}N. This result is consistent with year-round sediment trap measurements from the Bransfield Basin (Antarctica), with lowest $\delta^{15}N$ values during the productive season and increasing enrichment towards winter (Khim et al. 2013).

Bloom and vertical flux patterns are highly seasonal in the Arctic (Wassmann et al., 2006; Leu et al., 2011; Leu et al., 2015), which can lead to different timing of seasonal stages at different locations, depending on the sea ice cover. Accordingly, revisiting the same transect revealed advanced and delayed seasonalities at each of the stations within the same sampling campaign. This was especially evident in May.

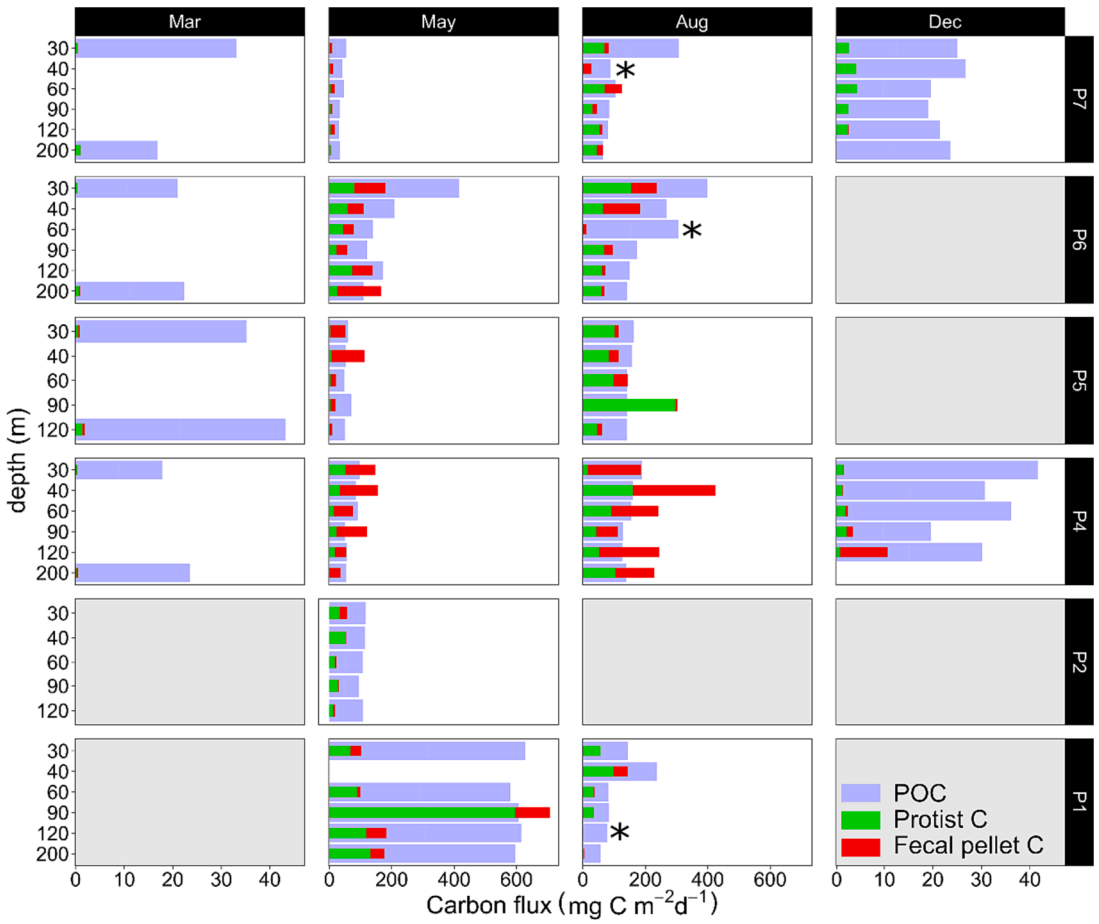

Fig. 5. Composition of vertical flux across all seasons and stations in the northwestern Barents Sea. Thick blue bars show the total POC, overlying green and red bars show the estimated contributions of protist (PC) and fecal pellet carbon (FPC), respectively. Note that for PC and FPC, carbon conversions can sometimes lead to overestimates, leading to estimations > 100% of total POC. * No PC data available from August P1-120 m, P6-60 m and P7-40 m. Note the different scales on the x-axes.

POC fluxes ranging between ~ 30 and 600 mg C m^{-2} d^{-1} in May are in accordance with previously shown high spatial variability in spring within the region, though our range is lower than previously reported (~100 – 870 mg C m^{-2} d^{-1}, Reigstad et al., 2008; 200 – 1500 mg C m^{-2} d^{-1}, Olli et al., 2002; and 400 – 1100 mg C m^{-2} d^{-1} below 100 m, Andreassen & Wassmann, 1998; Wassmann, 1998). While the southernmost station P1 displayed the highest fluxes measured during all seasons, fluxes at the northernmost station P7 were similar to those in March (Figs. 2, 8) or during the pre-bloom period in the same area (Olli et al., 2002) and North of Svalbard (Dybwad et al., 2021). This suggests that during our sampling time in May, "spring" had started in the southern part of the transect (P1), while P7 was still in a "winter" pre-bloom state. Spring blooms often follow the northward retreat of the sea ice, with southern stations experiencing local blooms along the MIZ earlier in the year (Wassmann, 2018; Castro de la Guardia et al., 2023; this issue). The ice edge reached all the way to P2 in May, reducing incident light for primary production further north, although nutrients were abundant at the surface (Figure S3, Jones et al., 2023; this issue). By contrast, we observed highest fluxes at P1, which was not ice-covered. In the northern Barents Sea, "spring" (i.e. early and peak bloom conditions), occurs from mid-May until July, depending on sea-ice conditions (Reigstad et al., 2008). Accordingly, the timing of sampling in May certainly resulted in a wide span in pelagic conditions and characteristic fluxes, from spring bloom to winter pre-bloom regimes. By contrast, the highest vertical flux along the transect during August was present at the northernmost stations P6 and P7, while lowest fluxes were measured at the southernmost station P1, consistent with the northward retreat of the sea ice edge. Accordingly, May and August framed the start and the end of a productive period in the northern Barents Sea, as May displayed early spring and August late summer conditions.

In general, vertical flux patterns of OM became more uniform across the different locations in August compared to May (means of 159 ± 97 and 178 ± 199 mg C m^{-2} d^{-1} across the transect, respectively; Fig. 2). In May, the high range of Chl-*a* flux, Chl-*a*:Phaeo ratios, Chl-*a*:POC ratios (Fig. 5) and the δ^{13}C variation, when station locations were clearly separated along a wide range on the δ^{13}C axis (Fig. 4; range of 8.46 ‰), demonstrate a high spatial and compositional variability of vertical flux patterns during spring. Over the course of the season and increasingly open water area, this variability among stations is reduced. In August, δ^{13}C variation already had a smaller range of 5.72 ‰ and POC fluxes across the transect were more comparable (Fig. 5). It is also evident from the close grouping of the stations in the multivariate data visualizations during summer compared to their large distance during May (Figs. 7 and 8). Highest integrated suspended stocks of POC were observed across the transect during August (Fig. 8b; Marquardt et al., 2022a; Marquardt et al., 2022d), although vertical flux was not higher in this month compared to May. This suggests that a smaller fraction of the suspended OM is sinking in August compared to May, and with that a less efficient export of OM in summer. However, it also demonstrates that bulk export was sustained under summer conditions, even though the composition of vertical flux differed between the two seasons. Early and peak phytoplankton bloom conditions in spring usually lead to short, but intense diatom-driven export events of OM along the MIZ, in contrast to post-bloom scenarios in summer when the open water area is extended, nutrients are depleted and smaller,

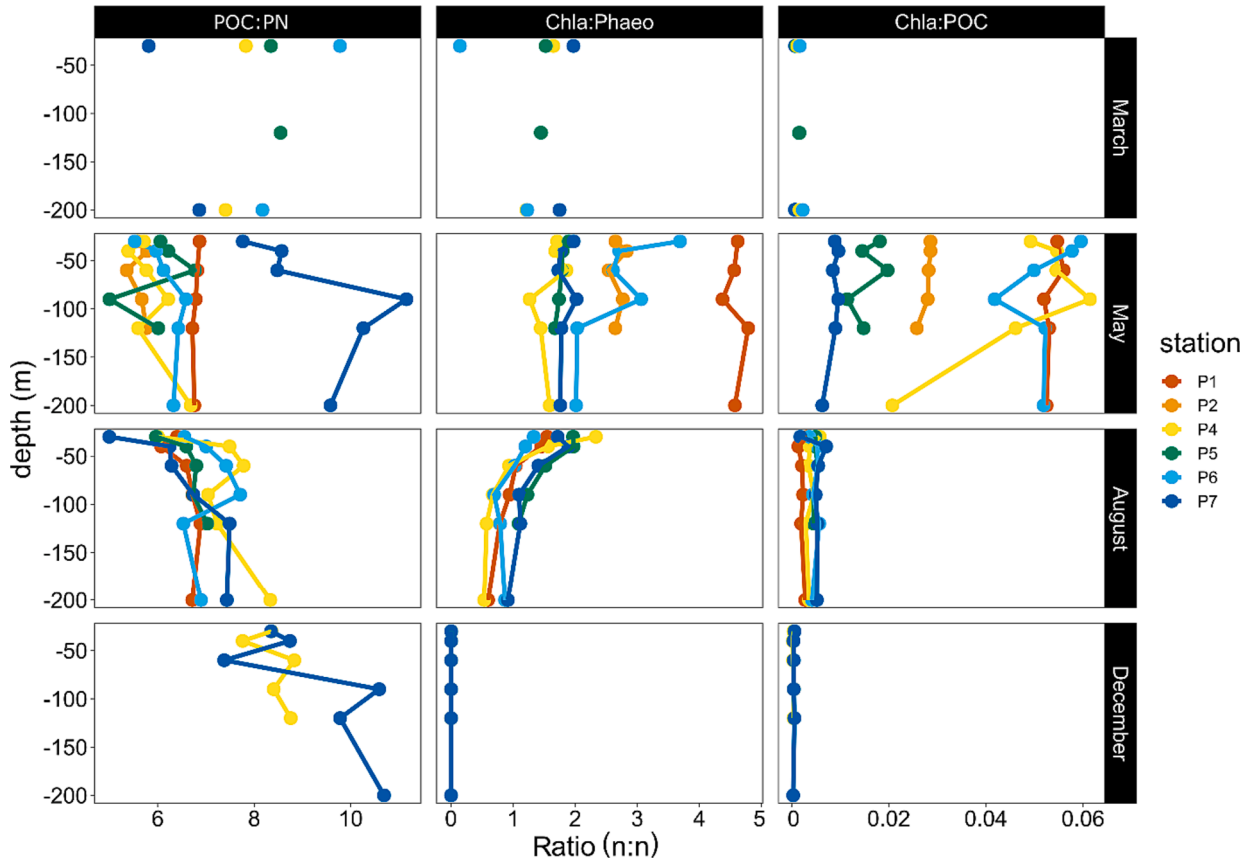

Fig. 6. POC:PN (left), Chl-a:Phaeopigments (mid) and Chl-a:POC ratios (right panel) of vertical flux across all seasons (facets) and stations (colors) in the northwestern Barents Sea.

less efficiently sinking cells dominate in the pelagic environment (Olli et al., 2002; Reigstad et al., 2008; Dybwad et al., 2021). While fluxes in May were strongly driven by large cells (Figure S1) and fresh Chl-*a* -rich material, fluxes in August were driven by high fecal pellet and small heterotrophic protist cell fluxes (Figs. S2, 8a). Small and presumably less efficiently sinking cells can contribute significantly to POC fluxes if they are abundant enough (Wiedmann et al., 2014) or packaged into fast-sinking fecal pellets (Wexels Riser et al., 2007; Dybwad et al., 2021). Even with progressing season, while the protist composition of vertical flux changes and protist carbon flux decreases (Kohlbach et al., 2023, this issue), bulk export can be sustained by detritus (and potentially fecal pellets) if sufficiently enough material escapes retention processes in the water column (Wassmann et al., 2003; Amargant-Arumí et al., this issue).

4.2. *High vertical flux under pack ice in early spring*

Vertical flux patterns during May did not strictly follow a latitudinal gradient consistent with the sea ice cover, as high fluxes at P6 under pack ice demonstrate. Similar to P1, at P6 high Chl-*a* fluxes were strongly associated with diatoms and were reflected in the high % Chl-*a* > 10 µm and high Chl-*a*:Phaeo ratios, indicating fresh material from a sinking diatom bloom (Fig. 7a and 8). At both P1 and P6, we also measured the least negative $\delta^{13}C$ values of ~ –22 ‰, which is in the range recorded earlier for $\delta^{13}C$ values in sinking OM in the Barents Sea under bloom conditions (~–21 ‰; Tamelander et al., 2009). In the early stage of a bloom, the lighter ^{12}C in dissolved inorganic caron (DIC) is quickly taken up, which leads to an accumulation of the heavier ^{13}C isotope in decreasing DIC concentrations as primary production continues. This is reflected in POM that becomes enriched in ^{13}C with increasing primary production (Rau et al., 1992).

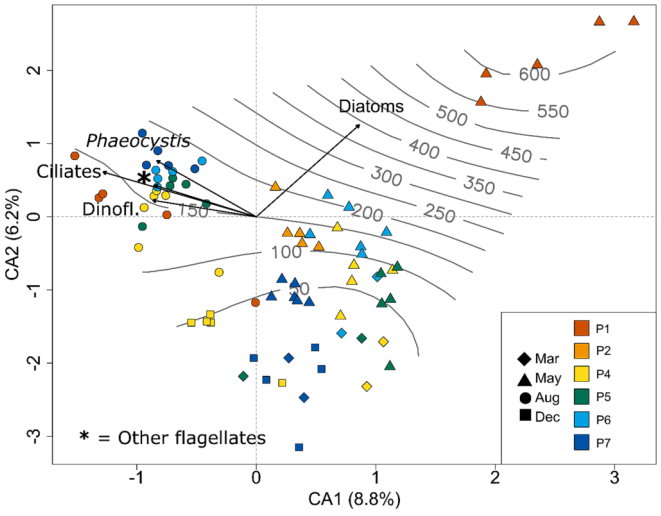

Fig. 7. Visualization of the Correspondence Analysis results on log-transformed protist cell fluxes (species level), with total cell fluxes of the different groups (Diatoms, Dinoflagellates, Ciliates, *Phaeocystis pouchetii* and other flagellates) plotted on top. Symbols represent seasons and colors represent stations. Isolines of POC fluxes are plotted on top of the ordination.

The AW inflow to the Arctic Ocean along the Barents Sea shelf break north of Svalbard may have led to favorable conditions for primary production at P6 early in the season. The heat of AW results in more fragile and mobile sea ice in this region, potentially leading to a higher occurrence of leads and large open-water areas (Onarheim et al., 2014; Ivanov et al., 2016; Renner et al., 2018). In fact, under-ice blooms are

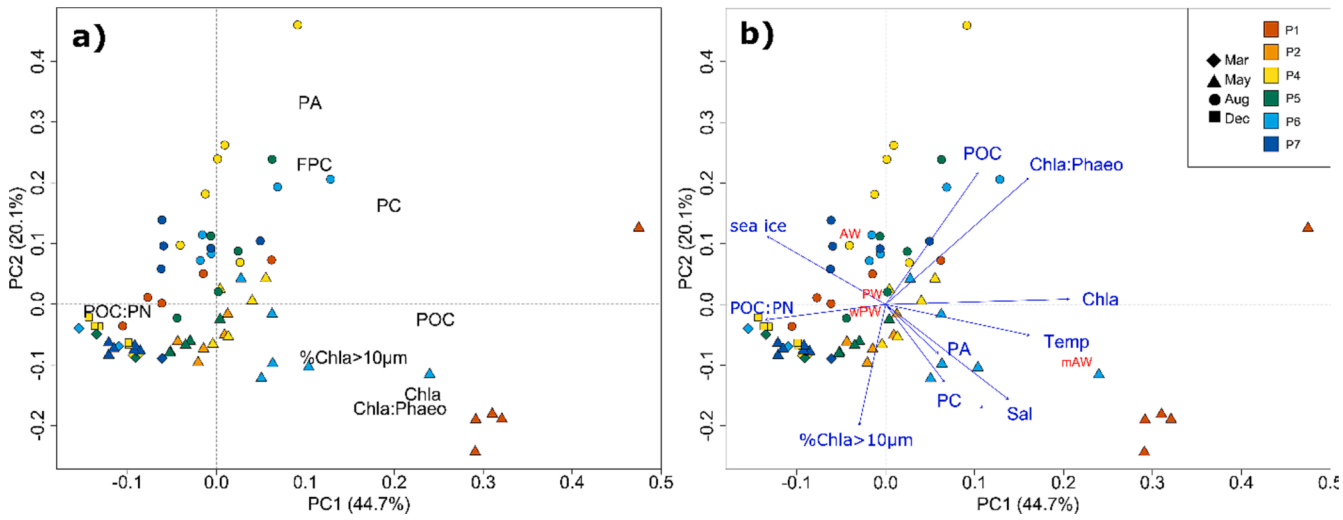

Fig. 8. Visualization of the Principal component analyses (PCA) performed on components of vertical flux from all seasons and stations. a) PCA of vertical flux components. POC = particulate organic carbon flux, POC:PN = POC to particulate nitrogen ratio, PA = protist abundance (cell flux), PC = protist carbon flux, FPC = fecal pellet carbon flux, Chla = Chlorophyll *a* flux, Chla:Phaeo = Chl-*a*:Phaeopigment ratio. b) PCA of vertical flux components (same as in a)), with environmental and suspended integrated biological parameters plotted on top. POC = integrated suspended particulate organic carbon, POC:PN = integrated suspended POC to particulate nitrogen ratio, PA = integrated suspended protist abundance, PC = integrated suspended protist carbon, Chla = integrated suspended Chlorophyll *a*, Chla:Phaeo = integrated suspended Chl-*a*:Phaeopigment ratio, % Chl-a > 10 µm = % of integrated suspended Chl-*a* > 10 µm, sea ice = mean sea ice concentration during one month before sampling. Water masses: AW = Atlantic water, mAW = modified AW, PW = Polar Water, wPW = warm PW.

observed under pack ice below meltponds or in leads, which are difficult to capture with satellite measurements (Assmy et al., 2017; Ardyna et al., 2020), although they can lead to subsequent vertical flux (Dybwad et al., 2021). Indeed, primary production measured locally was > 150 mg C m^{-2} d^{-1} during the time of the sediment trap deployment (pers. comm. Martí Amargant-Arumí, UiT The Arctic University of Norway), which is in the range of what has been measured earlier in the northern Barents Sea during spring blooms (Hegseth, 1998).

The community composition in the sediment traps at P6 suggests that a mix of ice-associated and pelagic diatoms were sinking at P6 in May. The ice-associated centric diatom *Thalassiosira bioculata* and pennate species such as *Nitzschia frigida, Fragilariopsis cylindricus* and *Navicula* spp. were present in sediment traps deployed 1 m below the sea ice at that station (Bodur et al., 2023l) as well as at 30 m. These ice-associated species were also present in the sea ice at this station (Marquardt et al., 2023, this issue). Below 60 m, pelagic diatoms such as *Chaetoceros furcillatus* dominated the community composition in the sediment traps. Moreover, there was a second peak in POC flux with higher Chl-*a*:Phaeo ratios at 120 m depth (Figs. 2 and 5). These findings suggest that the vertical flux at P6 may have originated from a mixture of a local under-ice bloom and an advected bloom. While it is difficult to disentangle the exact origin of sinking OM at this location, the patterns demonstrate that vertical flux in the northern Barents Sea does not strictly follow a northward retreating sea-ice gradient, but that the AW inflow and sea-ice cover drive its seasonality in concert, especially at the locations situated in the AW pathway (P1 and P6).

4.3. Vertical flux regulation by zooplankton: Fecal pellet flux and potential grazer mismatch

At several stations during May and August, we did not measure a typical attenuation curve of vertical flux (Martin et al., 1987). This could indicate that during the sediment trap deployments the OM was either remineralized above 30 m and we did not capture this, or OM was not degraded within the upper 100 m (Wassmann et al. 2003). At P1 during May, a possible mismatch between grazers and primary production could be the reason for high suspended standing stocks, high vertical flux of Chl-*a* and few identified fecal pellets down to 200 m. Indeed, zooplankton abundance and biomass was at a minimum in March and May, and lowest biomass during May were observed at P1 (Wold et al., 2023, this issue). A storm that simultaneously induced strong vertical mixing resulted in the transport of a high amount of ungrazed diatoms to, and probably below, 200 m depth, was most likely responsible for the lack of flux attentuation observed.

FPC contributions to POC fluxes were highest during summer and at the shelf stations north of the Polar Front (P4, P5), where we also noted a high amount of FP already at 30 m and little change of FPC flux with depth (Fig. 5), together with a lack of attenuation in POC fluxes (Fig. 2). Usually, vertical flux is attenuated within the upper 100 m (Wassmann et al., 2003), but these observations might indicate that high grazing pressure was already present above 30 m, leading to fast retention of OM at the surface and a subsequent lack of POC attenuation below this depth. Highest zooplankton abundance and biomass during summer (July and August) support this observation (Wold et al., 2023, this isue). FPC flux probably played an important role during summer when small cells that usually sink less efficiently are exported by packaging into fast-sinking fecal pellets (Turner, 2015; Wiedmann et al., 2016; von Appen et al., 2021). Highest seasonal POC fluxes can occur where there is a large contribution of FPC (Dybwad et al., 2021). Accordingly, FPC flux probably mediated an efficient export through packaging at these stations during summer when less efficiently sinking small flagellates and *Phaeocystis* dominated vertical flux (Fig. 8a, A2), or grazing reduced OM already above 30 m depth.

4.4. Elevated vertical flux at depth during March

During March, sinking OM below 100 m at the stations north of the Polar Front (P4, P5, P6) was highly enriched in ^{13}C and was within the range of the AW-influenced stations P1 and P6 during May, although POC fluxes below 45 mg C m^{-2} d^{-1} clearly mirrored a winter state. Moreover, Chl-*a* and POC fluxes at 120 and 200 m depth were slightly elevated relative to fluxes at 30 m. This indicates either resuspension from sediments or influence of different water masses at depth compared to the surface, since there was clearly no local vertical export of OM. Below 100 m, the presence of wPW (PW mixed with AW; after Sundfjord et al., 2020) could point towards an influence of AW at depth which shows elevated $\delta^{13}C$ values during early winter. In fact, AW is advected onto the northern Barents Sea shelf from the continental slope between

100 and 200 m and its inflow is seasonally highly variable, usually strongest between autumn and early March (Lundesgaard et al., 2022). The influence of this AW inflow probably became more conspicuous during March when compared to surface fluxes, since local biological processes are at their minima and would otherwise mask the $\delta^{13}C$ signal.

5. Summary and future implications

To the best of our knowledge, this study is the first that used short-term sediment traps along a revisited latitudinal transect during different seasons in order to investigate spatial and seasonal trends of daily vertical flux patterns in the seasonally ice-covered northwestern Barents Sea. Short-term sediment traps are particularly suited for investigating daily vertical flux (Buesseler et al., 2007; Baker et al., 2020); however, their use requires considerable ship time, is costly and especially challenging under ambient conditions in the Arctic.

We identified high spatial variability in vertical flux patterns in the northwestern Barents Sea region during early spring, spanning from peak bloom to late winter conditions, while with decreasing sea ice and increasing open water areas towards summer, vertical flux patterns became spatially more homogenous. These differences are driven by sea ice and the impact of AW, and led to the detection of high vertical flux events on the shelf break during both seasons. During late summer, higher concentrations of suspended POC but similar bulk fluxes compared to spring indicate a less efficient carbon pump. We suggest that fecal pellets played an important role for facilitating export during summer, leading to low attenuation of vertical flux at some stations below 30 m. During early spring, a wind-driven mixing event and a possible grazer mismatch led to an efficient transport of fresh OM down to at least 200 m. It should be noted that short-term deployments will not fully capture the seasonal cycle across such a large latitudinal gradient. Vertical fluxes of particulate organic matter during spring shown in this study were likely underestimated due to the ephemeral nature of the phytoplankton spring bloom. However, we were able to demonstrate (1) strong quantitative differences between the productive season in spring/summer and winter, and (2) differences in vertical flux composition between May and August.

With decreasing sea ice in the region, the northern Barents Sea will probably experience an earlier start of the summer season (Wassmann and Reigstad, 2011) with a less efficient carbon pump (i.e. a lower fraction of the suspended OM exported) and a higher contribution of *Phaeocystis*, flagellates and detritus to vertical flux. Nevertheless, a less efficient export over a prolonged productive season may still lead to high annual carbon export if vertical flux is sustained through the efficient packaging of small cells into fast-sinking fecal pellets or aggregates, and/or through mixing events.

The common notion that vertical flux strictly follows the sea-ice gradient and associated MIZ blooms is challenged, as vertical flux events under pack-ice might be common but are difficult to measure, especially in the region north of Svalbard where sea ice conditions are highly variable. With thinner ice cover and the increasing influence of AW, these export events are probably more likely to occur early in the season at locations still under consolidated ice cover before the onset of an MIZ bloom.

Declaration of Competing Interest

The authors declare that they have no known competing financial interests or personal relationships that could have appeared to influence the work reported in this paper.

Data availability

All data used for the research has been cited within the document.

Acknowledgements

We thank the captain and crew onboard RV “Kronprins Haakon” for invaluable support in the field, Paul Dubourg for POC analyses, Christine Dybwad for teaching the microscopic analysis of fecal pellets, Amanda Ziegler for support with stable isotope analyses, Elizabeth Jones for support with the allocation of water masses. This study was part of the Nansen Legacy project funded by the Research Council of Norway (#276730). Stable isotope samples were analyzed at the CLIPT stable isotope biogeochemistry lab at the University of Oslo, funded by the Research Council of Norway through its Centers of Excellence funding scheme #223272 (Centre for Earth Evolution and Dynamics). YVB was funded through UiT – the Arctic University of Norway.

Appendix A. Supplementary material

Supplementary data to this article can be found online at https://doi.org/10.1016/j.pocean.2023.103132.

References

Amargant-Arumí, M., Müller, O., Bodur, Y.V., Ntino, I.-V., Vonnahme, T., Assmy, P., Kohlbach, D., Chierici, M., Jones, E., Olsen, L.M., Tsagaraki, T.M., Reigstad, M., Bratbak, G., Gradinger, R. Interannual differences in sea ice regime in the northwestern Barents Sea cause major changes in summer pelagic production and export mechanisms. Prog. Oceanogr. (in review).

Andreassen, I., Wassmann, P., 1998. Vertical flux of phytoplankton and particulate biogenic matter in the marginal ice zone of the Barents Sea in May 1993. Mar. Ecol. Prog. Ser. 170 https://doi.org/10.3354/meps170001.

Ardyna, M., Mundy, C.J., Mayot, N., Matthes, L.C., Oziel, L., Horvat, C., Leu, E., Assmy, P., Hill, V., Matrai, P.A., Gale, M., Melnikov, I.A., Arrigo, K.R., 2020. Under-Ice Phytoplankton Blooms: Shedding Light on the “Invisible” Part of Arctic Primary Production. Front. Mar. Sci. 7 https://doi.org/10.3389/fmars.2020.608032.

Arrigo, K.R., van Dijken, G.L., 2015. Continued increases in Arctic Ocean primary production. Prog. Oceanogr. 136 https://doi.org/10.1016/j.pocean.2015.05.002.

Assmy, P., Fernández-Méndez, M., Duarte, P., Meyer, A., Randelhoff, A., Mundy, C.J., Olsen, L.M., Kauko, H.M., Bailey, A., Chierici, M., Cohen, L., Doulgeris, A.P., Ehn, J. K., Fransson, A., Gerland, S., Hop, H., Hudson, S.R., Hughes, N., Itkin, P., Johsen, G., King, J.A., Koch, B.P., Koenig, Z., Kwasniewski, S., Laney, S.R., Nicolaus, M., Pavlov, A.K., Polashenski, C.M., Provost, C., Rösel, A., Sandbu, M., Spreen, G., Smedsrud, L.H., Sundfjord, A., Taskjelle, T., Tatarek, A., Wiktor, J., Wagner, P.M., Wold, A., Steen, H., Granskog, M.A., 2017. Leads in Arctic pack ice enable early phytoplankton blooms below snow-covered sea ice. Sci. Rep. 7 https://doi.org/10.1038/srep40850.

Assmy, P., Gradinger, R., Edvardsen, B., Wiktor, J., Tatarek, A., Dąbrowska, A.M., 2022a. Phytoplankton biodiversity Nansen Legacy Q4. Norwegian Polar Institute. https://doi.org/10.21334/npolar.2022.5c40d100.

Assmy, P., Gradinger, R., Edvardsen, B., Wold, A., Goraguer, L., Wiktor, J., 2022b. Phytoplankton biodiversity Nansen Legacy Q1. Norwegian Polar Institute. https://doi.org/10.21334/npolar.2022.e6521515.

Assmy, P., Gradinger, R., Edvardsen, B., Wold, A., Goraguer, L., Wiktor, J., Tatarek, A., Dąbrowska, A.M., 2022c. Phytoplankton biodiversity Nansen Legacy Q3. Norwegian Polar Institute. https://doi.org/10.21334/npolar.2022.dadccf78.

Assmy, P., Gradinger, R., Edvardsen, B., Wold, A., Goraguer, L., Wiktor, J., Tatarek, A., Smoła, Z., 2022d. Phytoplankton biodiversity Nansen Legacy Q2. Norwegian Polar Institute. https://doi.org/10.21334/npolar.2022.9c05c643.

Baker, C.A., Estapa, M.L., Iversen, M., Lampitt, R., Buesseler, K., 2020. Are all sediment traps created equal? An intercomparison study of carbon export methodologies at the PAP-SO site. Prog. Oceanogr. 184 https://doi.org/10.1016/j.pocean.2020.102317.

Beszczynska-Möller, A., Fahrbach, E., Schauer, U., Hansen, E., 2012. Variability in Atlantic water temperature and transport at the entrance to the Arctic Ocean, 1997–2010. ICES J. Mar. Sci. 69 https://doi.org/10.1093/icesjms/fss056.

Bodur, Y.V., Amargant-Arumí, M., Reigstad, M., 2023a. Downward vertical flux of size-fractionated Chlorophyll-a and phaeopigments in the northern Barents Sea during August 2019, Nansen Legacy cruise 2019706 Q3. UiT The Arctic University of Norway. https://doi.org/10.11582/2023.00102.

Bodur, Y.V., Amargant-Arumí, M., Reigstad, M., 2023b. Downward vertical flux of size-fractionated Chlorophyll-a and phaeopigments in the northern Barents Sea during December 2019, Nansen Legacy cruise 2019711 Q4. UiT The Arctic University of Norway. https://doi.org/10.11582/2023.00103.

Bodur, Y.V., Amargant-Arumí, M., Reigstad, M., 2023c. Downward vertical flux of size-fractionated Chlorophyll-a and phaeopigments in the northern Barents Sea during March 2021, Nansen Legacy cruise 2021703 Q1. UiT The Arctic University of Norway. https://doi.org/10.11582/2023.00104.

Bodur, Y.V., Amargant-Arumí, M., Reigstad, M., 2023d. Downward vertical flux of size-fractionated Chlorophyll-a and phaeopigments in the northern Barents Sea during May 2021, Nansen Legacy cruise 2021704 Q2. UiT The Arctic University of Norway. https://doi.org/10.11582/2023.00105.

Bodur, Y.V., Amargant-Arumí, M., Reigstad, M., 2023e. Downward fecal pellet flux measured from short-term sediment traps during August 2019 in the northern Barents Sea as part of the Nansen Legacy project, cruise 2019706 Q3. UiT The Arctic University of Norway. https://doi.org/10.11582/2023.00108.
Bodur, Y.V., Amargant-Arumí, M., Reigstad, M., 2023f. Downward fecal pellet flux measured from short-term sediment traps during December in the northern Barents Sea as part of the Nansen Legacy project, cruise 2019711 Q4. UiT The Arctic University of Norway. https://doi.org/10.11582/2023.00106.
Bodur, Y.V., Amargant-Arumí, M., Reigstad, M., 2023g. Downward fecal pellet flux measured from short-term sediment traps during March 2021 in the northern Barents Sea as part of the Nansen Legacy project, cruise 2021703 Q1. UiT The Arctic University of Norway. https://doi.org/10.11582/2023.00086.
Bodur, Y.V., Amargant-Arumí, M., Reigstad, M., 2023h. Downward fecal pellet flux measured from short-term sediment traps during May 2021 in the northern Barents Sea as part of the Nansen Legacy project, cruise 2021704 Q2. UiT The Arctic University of Norway. https://doi.org/10.11582/2023.00107.
Bodur, Y.V., Dąbrowska, A.M., Tatarek, A., Wiktor, J.M., Goraguer, L., Amargant-Arumí, M., Reigstad, M., 2023i. Downward vertical flux of protist cells and biomass in the northern Barents Sea during August 2019, Nansen Legacy cruise 2019706 Q3. UiT The Arctic University of Norway. https://doi.org/10.11582/2023.00088.
Bodur, Y.V., Dąbrowska, A.M., Tatarek, A., Wiktor, J.M., Goraguer, L., Amargant-Arumí, M., Reigstad, M., 2023j. Downward vertical flux of protist cells and biomass in the northern Barents Sea during December 2019, Nansen Legacy cruise 2019711 Q4. UiT The Arctic University of Norway. https://doi.org/10.11582/2023.00089.
Bodur, Y.V., Dąbrowska, A.M., Tatarek, A., Wiktor, J.M., Goraguer, L., Amargant-Arumí, M., Reigstad, M., 2023k. Downward vertical flux of protist cells and biomass in the northern Barents Sea during March 2021, Nansen Legacy cruise 2021703 Q1. UiT The Arctic University of Norway. https://doi.org/10.11582/2023.00090.
Bodur, Y.V., Dąbrowska, A.M., Tatarek, A., Wiktor, J.M., Goraguer, L., Amargant-Arumí, M., Reigstad, M., 2023l. Downward vertical flux of protist cells and biomass in the northern Barents Sea during May 2021, Nansen Legacy cruise 2021704 Q2. UiT The Arctic University of Norway. https://doi.org/10.11582/2023.00091.
Bodur, Y.V., Marquardt, M., Dubourg, P., Amargant, M., Reigstad, M., 2023m. Downward vertical flux of particulate organic carbon (POC) and nitrogen (PON) in the northern Barents Sea during May 2021, Nansen Legacy cruise 2021704 Q2. UiT The Arctic University of Norway. https://doi.org/10.11582/2023.00096.
Bodur, Y.V., Marquardt, M., Dubourg, P., Amargant-Arumí, M., Reigstad, M., 2023n. Downward vertical flux of particulate organic carbon (POC) and nitrogen (PON) in the northern Barents Sea during August 2019, Nansen Legacy cruise 2019706 Q3. UiT The Arctic University of Norway. https://doi.org/10.11582/2023.00093.
Bodur, Y.V., Marquardt, M., Dubourg, P., Amargant-Arumí, M., Reigstad, M., 2023o. Downward vertical flux of particulate organic carbon (POC) and nitrogen (PON) in the northern Barents Sea during December 2019, Nansen Legacy cruise 2019711 Q4. UiT The Arctic University of Norway. https://doi.org/10.11582/2023.00094.
Bodur, Y.V., Marquardt, M., Dubourg, P., Amargant-Arumí, M., Reigstad, M., 2023p. Downward vertical flux of particulate organic carbon (POC) and nitrogen (PON) in the northern Barents Sea during March 2021, Nansen Legacy cruise 2021703 Q1. UiT The Arctic University of Norway. https://doi.org/10.11582/2023.00095.
Bodur, Y.V., Renaud, P.E., Amargant-Arumí, M., Reigstad, M., 2023q. Stable isotopic composition (d13C and d15N) of sinking particulate matter measured from short-term sediment traps in the northern Barents Sea during August 2019, Nansen Legacy cruise 2019706 Q3. UiT The Arctic University of Norway. https://doi.org/10.11582/2023.00097.
Bodur, Y.V., Renaud, P.E., Amargant-Arumí, M., Reigstad, M., 2023r. Stable isotopic composition (d13C and d15N) of sinking particulate matter measured from short-term sediment traps in the northern Barents Sea during December 2019, Nansen Legacy cruise 2019711 Q4. UiT The Arctic University of Norway. https://doi.org/10.11582/2023.00098.
Bodur, Y.V., Renaud, P.E., Amargant-Arumí, M., Reigstad, M., 2023s. Stable isotopic composition (d13C and d15N) of sinking particulate matter measured from short-term sediment traps in the northern Barents Sea during March 2021, Nansen Legacy cruise 2021703 Q1. UiT The Arctic University of Norway. https://doi.org/10.11582/2023.00099.
Bodur, Y.V., Renaud, P.E., Amargant-Arumí, M., Reigstad, M., 2023t. Stable isotopic composition (d13C and d15N) of sinking particulate matter measured from short-term sediment traps in the northern Barents Sea during May 2021, Nansen Legacy cruise 2021704 Q2. UiT The Arctic University of Norway. https://doi.org/10.11582/2023.00100.
Buesseler, K.N., Antia, A., Chen, M., Fowler, S., Gardner, W., Gustafsson, O., Harada, K., Michaels, A., van der Loeff, M.R., Sarin, M.M., Steinberg, D.K., Trull, T., 2007. An assessment of the use of sediment traps for estimating upper ocean particle fluxes. J. Mar. Res. 65 https://doi.org/10.1357/002224007781567621.
Carroll, J., Zaborska, A., Papucci, C., Schirone, A., Carroll, M.L., Pempkowiak, J., 2008. Accumulation of organic carbon in western Barents Sea sediments. Deep Sea Res. Part II 55. https://doi.org/10.1016/j.dsr2.2008.05.005.
Castro de la Guardia, L., Hernández Fariñas, T., Marchese, C., Amargant-Arumí, M., Myers, P.G., Bélanger, S., Assmy, P., Gradinger, R.R., Duarte, P., 2023. Assessing net primary production in the northwestern Barents Sea using in situ, remote sensing and modelling approaches. Prog. Oceanogr. (under review).
Dalpadado, P., Ingvaldsen, R.B., Stige, L.C., Bogstad, B., Knutsen, T., Ottersen, G., Ellertsen, B., 2012. Climate effects on Barents Sea ecosystem dynamics. ICES J. Mar. Sci. 69 https://doi.org/10.1093/icesjms/fss063.
Dalpadado, P., Arrigo, K.R., Hjøllo, S.S., Rey, F., Ingvaldsen, R.B., Sperfeld, E., van Dijken, G.L., Stige, L.C., Olsen, A., Ottersen, G., 2014. Productivity in the Barents Sea - response to recent climate variability. PLoS One 9. https://doi.org/10.1371/journal.pone.0095273.
De La Rocha, C.L., Passow, U., 2007. Factors influencing the sinking of POC and the efficiency of the biological carbon pump. Deep Sea Res. Part II 54. https://doi.org/10.1016/j.dsr2.2007.01.004.
Dezutter, T., Lalande, C., Darnis, G., Fortier, L., 2021. Seasonal and interannual variability of the Queen Maud Gulf ecosystem derived from sediment trap measurements. Limnol. Oceanogr. 66 https://doi.org/10.1002/lno.11628.
Dilling, L., Alldredge, A., 1993. Can chaetognath fecal pellets contribute significantly to carbon flux? Mar. Ecol. Prog. Ser. 92 https://doi.org/10.3354/meps092051.
Drinkwater, K.F., 2011. The influence of climate variability and change on the ecosystems of the Barents Sea and adjacent waters: review and synthesis of recent studies from the NESSAS Project. Prog. Oceanogr. 90 https://doi.org/10.1016/j.pocean.2011.02.006.
Dybwad, C., Assmy, P., Olsen, L.M., Peeken, I., Nikolopoulos, A., Krumpen, T., Randelhoff, A., Tatarek, A., Wiktor, J.M., Reigstad, M., 2021. Carbon export in the seasonal sea ice zone north of Svalbard from winter to late summer. Front. Mar. Sci. 7 https://doi.org/10.3389/fmars.2020.525800.
Dybwad, C., Lalande, C., Bodur, Y.V., Henley, S.F., Cottier, F., Ershova, E.A., Hobbs, L., Last, K.S., Dąbrowska, A.M., Reigstad, M., 2022. The influence of sea ice cover and Atlantic Water advection on annual particle export north of Svalbard. J. Geophys. Res. Oceans 127. https://doi.org/10.1029/2022JC018897.
Edler, L., Elbrächter, M., 2010. The Utermöhl method for quantitative phytoplankton analysis. In: Microscopic and Molecular Methods for Quantitative Phytoplankton Analysis. Unesco Pub, pp. 13–20.
Ellingsen, I.H., Dalpadado, P., Slagstad, D., Loeng, H., 2008. Impact of climatic change on the biological production in the Barents Sea. Clim. Change 87. https://doi.org/10.1007/s10584-007-9369-6.
Eriksen, E., Skjoldal, H.R., Gjøsæter, H., Primicerio, R., 2017. Spatial and temporal changes in the Barents Sea pelagic compartment during the recent warming. Prog. Oceanogr. 151 https://doi.org/10.1016/j.pocean.2016.12.009.
Fadeev, E., Rogge, A., Ramondenc, S., Nöthig, E.-M., Wekerle, C., Bienhold, C., Salter, I., Waite, A.M., Hehemann, L., Boetius, A., Iversen, M.H., 2021. Sea ice presence is linked to higher carbon export and vertical microbial connectivity in the Eurasian Arctic Ocean. Commun. Biol. 4 https://doi.org/10.1038/s42003-021-02776-w.
Fossheim, M., Primicerio, R., Johannesen, E., Ingvaldsen, R.B., Aschan, M.M., Dolgov, A. V., 2015. Recent warming leads to a rapid borealization of fish communities in the Arctic. Nat. Clim. Chang. 5 https://doi.org/10.1038/nclimate2647.
Franco-Santos, R.M., Auel, H., Boersma, M., De Troch, M., Meunier, C.L., Niehoff, B., 2018. Bioenergetics of the copepod Temora longicornis under different nutrient regimes. J. Plankton Res. 40 https://doi.org/10.1093/plankt/fby016.
Gerland, S., 2022. CTD data from Nansen Legacy Cruise - Seasonal Cruise Q1. Norwegian Polar Institute. https://doi.org/10.21335/NMDC-1491279668.
Giesecke, R., González, H.E., Bathmann, U., 2010. The role of the chaetognath Sagitta gazellae in the vertical carbon flux of the Southern Ocean. Polar Biol. 33 https://doi.org/10.1007/s00300-009-0704-4.
Hegseth, E.N., 1998. Primary production of the northern Barents Sea. Polar Res. 17 https://doi.org/10.1111/j.1751-8369.1998.tb00266.x.
Hillebrand, H., Dürselen, C.-D., Kirschtel, D., Pollingher, U., Zohary, T., 1999. Biovolume calculation for pelagic and benthic microalgae. J. Phycol. 35 https://doi.org/10.1046/j.1529-8817.1999.3520403.x.
Holm-Hansen, O., Riemann, B., 1978. Chlorophyll a determination: Improvements in methodology. Oikos 30. https://doi.org/10.2307/3543338.
Ingvaldsen, R.B., Asplin, L., Loeng, H., 2004. The seasonal cycle in the Atlantic transport to the Barents Sea during the years 1997–2001. Cont. Shelf Res. 24 https://doi.org/10.1016/j.csr.2004.02.011.
Ingvaldsen, R.B., Assmann, K.M., Primicerio, R., Fossheim, M., Polyakov, I.V., Dolgov, A, V., 2021. Physical manifestations and ecological implications of Arctic Atlantification. Nat. Rev. Earth. Environ. 2. Nature Publishing Group. https://doi.org/10.1038/s43017-021-00228-x.
Ingvaldsen, R., Loeng, H., Asplin, L., 2002. Variability in the Atlantic inflow to the Barents Sea based on a one-year time series from moored current meters. Cont. Shelf Res. 22 https://doi.org/10.1016/S0278-4343(01)00070-X.
Ivanov, V., Alexeev, V., Koldunov, N.V., Repina, I., Sandø, A.B., Smedsrud, L.H., Smirnov, A., 2016. Arctic Ocean heat impact on regional ice decay: A suggested positive feedback. J. Geophys. Res. Oceans 46. https://doi.org/10.1175/JPO-D-15-0144.1.
Iversen, M.H., 2023. Carbon export in the ocean: a biologist's perspective. Annu Rev Mar Sci 15. https://doi.org/10.1146/annurev-marine-032122-035153.
Jakobsson, M., Mayer, L.A., Bringensparr, C., Castro, C.F., Mohammad, R., Johnson, P., Ketter, T., Accettella, D., Amblas, D., An, L., Arndt, J.E., Canals, M., Casamor, J.L., Chauché, N., Coakley, B., Danielson, S., Demarte, M., Dickson, M.-L., Dorschel, B., Dowdeswell, J.A., Dreutter, S., Fremand, A.C., Gallant, D., Hall, J.K., Hehemann, L., Hodnesdal, H., Hong, J., Ivaldi, R., Kane, E., Klaucke, I., Krawczyk, D.W., Kristoffersen, Y., Kuipers, B.R., Millan, R., Masetti, G., Morlighem, M., Noormets, R., Prescott, M.M., Rebesco, M., Rignot, E., Semiletov, I., Tate, A.J., Travaglini, P., Velicogna, I., Weatherall, P., Weinrebe, W., Willis, J.K., Wood, M., Zarayskaya, Y., Zhang, T., Zimmermann, M., Zinglersen, K.B., 2020. The International Bathymetric Chart of the Arctic Ocean Version 4.0. Sci. Data 7. https://doi.org/10.1038/s41597-020-0520-9.
Jones, E.M., Chierici, M., Fransson, A., Assmann, K.M., Renner, A.H.H., Lødemel, H.H., 2023. Inorganic carbon and nutrient dynamics in the marginal ice zone of the Barents Sea: seasonality and implications for ocean acidification. Prog. Oceanogr. (Journal Preprint). https://doi.org/10.1016/j.pocean.2023.103131.
Khim, B.-K., Dunbar, R., Kim, D., 2013. δ15N values of settling biogenic particles in the eastern Bransfield Basin (west Antarctic) and their records for the surface-water condition. Geosci. J. 17 https://doi.org/10.1007/s12303-013-0032-0.

Koch, C.W., Cooper, L.W., Lalande, C., Brown, T.A., Frey, K.E., Grebmeier, J.M., 2020. Seasonal and latitudinal variations in sea ice algae deposition in the Northern Bering and Chukchi Seas determined by algal biomarkers. PLOS ONE 15. https://doi.org/10.1371/journal.pone.0231178. Public Library of Science.

Kohlbach, D., Goraguer, L., Bodur, Y.V., Müller, O., Amargant-Arumí, M., Blix, K., Bratbak, G., Chierici, M., Maria Dąbrowska, A., Dietrich, U., Edvardsen, B., García, L. M., Gradinger, R., Hop, H., Jones, E., Lundesgaard, Ø., Olsen, L.M., Reigstad, M., Saubrekka, K., Tatarek, A., Wiktor, J., Wold, A., Philipp, A., 2023. Earlier sea-ice melt extends the oligotrophic summer period in the Barents Sea with low algal biomass and associated low vertical flux. Prog. Oceanogr. 213 https://doi.org/10.1016/j.pocean.2023.103018.

Lalande, C., Moriceau, B., Leynaert, A., Morata, N., 2016a. Spatial and temporal variability in export fluxes of biogenic matter in Kongsfjorden. Polar Biol. 39 https://doi.org/10.1007/s00300-016-1903-4.

Lalande, C., Nöthig, E.-M., Bauerfeind, E., Hardge, K., Beszczynska-Möller, A., Fahl, K., 2016b. Lateral supply and downward export of particulate matter from upper waters to the seafloor in the deep eastern Fram Strait. Deep Sea Res. Part I Oceanogr. 114 https://doi.org/10.1016/j.dsr.2016.04.014.

Leu, E., Søreide, J., Hessen, D., Falk-Petersen, S., Berge, J., 2011. Consequences of changing sea-ice cover for primary and secondary producers in the European Arctic shelf seas: timing, quantity, and quality. Prog. Oceanogr. 90 https://doi.org/10.1016/j.pocean.2011.02.004.

Leu, E., Mundy, C.J., Assmy, P., Campbell, K., Gabrielsen, T.M., Gosselin, M., Juul-Pedersen, T., Gradinger, R., 2015. Arctic spring awakening – steering principles behind the phenology of vernal ice algal blooms. Prog. Oceanogr. 139 https://doi.org/10.1016/j.pocean.2015.07.012.

Lewis, K.M., van Dijken, G.L., Arrigo, K.R., 2020. Changes in phytoplankton concentration now drive increased Arctic Ocean primary production. Science 369. https://doi.org/10.1126/science.aay8380.

Lind, S., Ingvaldsen, R.B., 2012. Variability and impacts of Atlantic Water entering the Barents Sea from the north. Deep Sea Res Part I Oceanogr 62. https://doi.org/10.1016/j.dsr.2011.12.007.

Ludvigsen, M., 2022. CTD data from Nansen Legacy Cruise - Seasonal cruise Q2. University Centre in Svalbard. https://doi.org/10.21335/NMDC-515075317.

Lundesgaard, Ø., Sundfjord, A., Lind, S., Nilsen, F., Renner, A.H.H., 2022. Import of Atlantic Water and sea ice controls the ocean environment in the northern Barents Sea. Ocean Sci. 18 https://doi.org/10.5194/os-18-1389-2022.

Manno, C., Stowasser, G., Enderlein, P., Fielding, S., Tarling, G.A., 2015. The contribution of zooplankton faecal pellets to deep-carbon transport in the Scotia Sea (Southern Ocean). Biogeosci. 12 https://doi.org/10.5194/bg-12-1955-2015.

Marquardt, M., Bodur, Y.V., Dubourg, P., Reigstad, M., 2022a. Concentration of particulate organic carbon (POC) and particulate organic nitrogen (PON) from the sea water and sea ice in the northern Barents Sea as part of the Nansen Legacy project, Cruise 2019706 Q3. UiT The Arctic University of Norway. https://doi.org/10.11582/2022.00055.

Marquardt, M., Bodur, Y.V., Dubourg, P., Reigstad, M., 2022b. Concentration of Particulate Organic Carbon (POC) and Particulate Organic Nitrogen (PON) from the sea water and sea ice in the northern Barents Sea as part of the Nansen Legacy project, Cruise 2019711 Q4. UiT The Arctic University of Norway. https://doi.org/10.11582/2022.00048.

Marquardt, M., Bodur, Y.V., Dubourg, P., Reigstad, M., 2022c. Concentration of Particulate Organic Carbon (POC) and Particulate Organic Nitrogen (PON) from the sea water and sea ice in the northern Barents Sea as part of the Nansen Legacy project, Cruise 2021703 Q1. UiT The Arctic University of Norway. https://doi.org/10.11582/2022.00053.

Marquardt, M., Bodur, Y.V., Dubourg, P., Reigstad, M., 2022d. Concentration of Particulate Organic Carbon (POC) and Particulate Organic Nitrogen (PON) from the sea water and sea ice in the northern Barents Sea as part of the Nansen Legacy project, Cruise 2021704 Q2. UiT The Arctic University of Norway. https://doi.org/10.11582/2022.00054.

Marquardt, M., Goraguer, L., Assmy, P., Bluhm, B.A., Aaboe, S., Down, E., Patrohay, E., Edvardsen, B., Tatarek, A., Smoła, S., Wiktor, J., Gradinger, R., 2023. Seasonal Dynamics of Sea-Ice Protist and Meiofauna in the Northwestern Barents Sea. Prog. Oceanogr. (Journal Preprint). https://doi.org/10.1016/j.pocean.2023.103128.

Martin, J.H., Knauer, G.A., Karl, D.M., Broenkow, W.W., 1987. VERTEX: carbon cycling in the northeast Pacific. Deep Sea Res Part I Oceanogr 34. https://doi.org/10.1016/0198-0149(87)90086-0.

Menden-Deuer, S., Lessard, E.J., 2000. Carbon to volume relationships for dinoflagellates, diatoms, and other protist plankton. Limnol. Oceanogr. 45 https://doi.org/10.4319/lo.2000.45.3.0569.

Mousing, E.A., Ellingen, I., Hjøllo, S.S., Husson, B., Skogen, M.D., Wallhead, P., 2023. Why do regional biogeochemical models produce contrasting future projections of primary production in the Barents Sea? J. Sea Res. 192, 102366 https://doi.org/10.1016/j.seares.2023.102366.

Oksanen, J,, Blanchet, F,G,, Friendly, M., Kindt, R., Legendre, P., McGlinn, D., Minchin, P.R., O'Hara, R.B., Simpson, G.L., Solymos, P,, et al., 2018. vegan: Community Ecology Package. Available at https://CRAN.R-project.org/package=vegan. Accessed 2018 Aug 22.

Nöthig, E.-M., Bracher, A., Engel, A., Metfies, K., Niehoff, B., Peeken, I., Bauerfeind, E., Cherkasheva, A., Gäbler-Schwarz, S., Hardge, K., Kilias, E., Kraft, A., Kidane, Y.M., Lalande, C., Piontek, J., Thomisch, K., Wurst, M., 2015. Summertime plankton ecology in Fram Strait—a compilation of long- and short-term observations. Polar Res. 34 https://doi.org/10.3402/polar.v34.23349.

Olli, K., Wexels Riser, C., Wassmann, P., Ratkova, T., Arashkevich, E., Pasternak, A., 2002. Seasonal variation in vertical flux of biogenic matter in the marginal ice zone and the central Barents Sea. J. Mar. Syst. 38 https://doi.org/10.1016/S0924-7963(02)00177-X.

Onarheim, I.H., Teigen, S.H., 2018. Statistical position of the oceanic polar front in the Barents Sea. Equinor. Barents Sea Exploration Collaboration (BaSEC) report Report No.: MAD-RE2018-016. Available at https://offshorenorge.no/globalassets/dokumenter/miljo/barents-sea-exploration-collaboration/basec-rapport-11-hvor-er-polarfronten.pdf. Accessed 2023 Jan 30.

Onarheim, I.H., Eldevik, T., Smedsrud, L.H., Stroeve, J.C., 2018. Seasonal and regional manifestation of arctic sea ice loss. J. Clim. 31 https://doi.org/10.1175/JCLI-D-17-0427.1.

Onarheim, I.H., Smedsrud, L.H., Ingvaldsen, R.B., Nilsen, F., 2014. Loss of sea ice during winter north of Svalbard. Tellus A: Dyn. Meteorol. Oceanogr. 66 https://doi.org/10.3402/tellusa.v66.23933.

Oziel, L., Baudena, A., Ardyna, M., Massicotte, P., Randelhoff, A., Sallée, J.-B., Ingvaldsen, R.B., Devred, E., Babin, M., 2020. Faster Atlantic currents drive poleward expansion of temperate phytoplankton in the Arctic Ocean. Nat. Commun. 11 https://doi.org/10.1038/s41467-020-15485-5.

Peterson, B.J., Fry, B., 1987. Stable isotopes in ecosystem studies. Annu. Rev. Ecol. Evol. Syst. 18. http://www.jstor.org/stable/2097134 (Accessed 2022 Nov 16).

Polyakov, I.V., Alkire, M.B., Bluhm, B.A., Brown, K.A., Carmack, E.C., Chierici, M., Danielson, S.L., Ellingsen, I., Ershova, E.A., Gårdfeldt, K., Ingvaldsen, R.B., Pnyushkov, A.V., Slagstad, D., Wassmann, P., 2020. Borealization of the Arctic Ocean in response to anomalous advection from sub-arctic seas. Front. Mar. Sci. 7 https://doi.org/10.3389/fmars.2020.00491.

Rau, G.H., Takahashi, T., Des Marais, D.J., Repeta, D.J., Martin, J.H., 1992. The relationship between δ13C of organic matter and [CO2(aq)] in ocean surface water: Data from a JGOFS site in the northeast Atlantic Ocean and a model. Geochim. Cosmochim. Acta 56. https://doi.org/10.1016/0016-7037(92)90073-R.

Reigstad, M., 2022. CTD data from Nansen Legacy Cruise - Seasonal cruise Q3. UiT The Arctic University of Tromsø https://doi.org/10.21335/NMDC-1107597377.

Reigstad, M., Wexels Riser, C., Wassmann, P., Ratkova, T., 2008. Vertical export of particulate organic carbon: Attenuation, composition and loss rates in the northern Barents Sea. Deep Sea Res. Part II 55. https://doi.org/10.1016/j.dsr2.2008.05.007.

Renaud, P.E., Daase, M., Banas, N.S., Gabrielsen, T.M., Søreide, J.E., Varpe, Ø., Cottier, F., Falk-Petersen, S., Halsband, C., Vogedes, D., Heggland, K., Berge, J., 2018. Pelagic food-webs in a changing Arctic: a trait-based perspective suggests a mode of resilience. ICES J. Mar. Sci. 75 https://doi.org/10.1093/icesjms/fsy063.

Renner, A.H.H., Sundfjord, A., Janout, M.A., Ingvaldsen, R.B., Beszczynska-Möller, A., Pickart, R.S., Pérez-Hernández, M.D., 2018. Variability and redistribution of heat in the Atlantic Water boundary current north of Svalbard. J. Geophys. Res. Oceans 123. https://doi.org/10.1029/2018JC013814.

Riebesell, U., Reigstad, M., Wassmann, P., Noji, T., Passow, U., 1995. On the trophic fate of Phaeocystis pouchetii (hariot): VI. Significance of Phaeocystis-derived mucus for vertical flux. Neth J. Sea Res. 33 https://doi.org/10.1016/0077-7579(95)90006-3.

Rousseau, V., Mathot, S., Lancelot, C., 1990. Calculating carbon biomass ofPhaeocystis sp. from microscopic observations. Mar. Biol. 107 https://doi.org/10.1007/BF01319830.

Sakshaug, E., Johnsen, G., Kristiansen, S., von Quillfeldt, C.H., Rey, F., Slagstad, D., Thingstad, F., 2009. Phytoplankton and Primary Production. In: Sakshaug, E., Johnsen, G., Kovacs, K.M. (Eds.), Ecosystem Barents Sea. Tapir Academic Press, Trondheim, pp. 167–208.

Screen, J.A., Simmonds, I., 2010. Increasing fall-winter energy loss from the Arctic Ocean and its role in Arctic temperature amplification. Geophys. Res. Lett. 37 https://doi.org/10.1029/2010GL044136.

Skagseth, Ø., Eldevik, T., Årthun, M., Asbjørnsen, H., Lien, V.S., Smedsrud, L.H., 2020. Reduced efficiency of the Barents Sea cooling machine. Nat. Clim. Chang. 10 https://doi.org/10.1038/s41558-020-0772-6.

Slagstad, D., Ellingsen, I.H., Wassmann, P., 2011. Evaluating primary and secondary production in an Arctic Ocean void of summer sea ice: An experimental simulation approach. Prog. Oceanogr. 90 https://doi.org/10.1016/j.pocean.2011.02.009.

Slagstad, D., Wassmann, P.F.J., Ellingsen, I., 2015. Physical constrains and productivity in the future Arctic Ocean. Front. Mar. Sci. 2 https://doi.org/10.3389/fmars.2015.00085.

Smedsrud, L.H., Muilwijk, M., Brakstad, A., Madonna, E., Lauvset, S.K., Spensberger, C., Born, A., Eldevik, T., Drange, H., Jeansson, E., Li, C., Olsen, A., Skagseth, Ø., Slater, D.A., Straneo, F., Våge, K., Årthun, M., 2022. Nordic Seas Heat Loss, Atlantic Inflow, and Arctic Sea Ice Cover Over the Last Century. Rev. Geophys. 60 https://doi.org/10.1029/2020RG000725.

Søreide, J., 2022. CTD data from Nansen Legacy Cruise - Seasonal cruise Q4. University Centre in Svalbard. https://doi.org/10.21335/NMDC-301551919.

Steer, A., Divine, D., 2023. Sea ice concentrations in the northern Barents Sea and the area north of Svalbard at Nansen Legacy stations during 2017–2021. Norwegian Polar Institute. https://doi.org/10.21334/NPOLAR.2023.24F2939C.

Sundfjord, A., Assmann, K.M., Lundesgaard, Ø., Renner, A.H.H., Lind, S., Ingvaldsen, R. B., 2020. Suggested water mass definitions for the central and northern Barents Sea, and the adjacent Nansen Basin: Workshop Report. Report No. 8 https://doi.org/10.7557/nlrs.5707.

Tamelander, T., Kivimäe, C., Bellerby, R.G.J., Renaud, P.E., Kristiansen, S., 2009. Baseline variations in stable isotope values in an Arctic marine ecosystem: effects of carbon and nitrogen uptake by phytoplankton. Hydrobiologia 630. https://doi.org/10.1007/s10750-009-9780-2.

Trudnowska, E., Lacour, L., Ardyna, M., Rogge, A., Irisson, J.O., Waite, A.M., Babin, M., Stemmann, L., 2021. Marine snow morphology illuminates the evolution of phytoplankton blooms and determines their subsequent vertical export. Nat. Commun. 12 https://doi.org/10.1038/s41467-021-22994-4.

Turner, J.T., 2015. Zooplankton fecal pellets, marine snow, phytodetritus and the ocean's biological pump. Prog. Oceanogr. 130 https://doi.org/10.1016/j.pocean.2014.08.005.

Urban-Rich JL. 1997. Latitudinal variations in the contribution by copepod fecal pellets to organic carbon and amino acid flux. [Ann Arbor, United States]: University of Maryland. Available at https://www.proquest.com/docview/304350779/abstract/451E5A796DF848E3PQ/1. Accessed 2022 Oct 8.

Utermöhl, H., 1958. Zur Vervollkommnung der quantitativen Phytoplankton-Methodik. SIL Communications 1953–1996, 9. https://doi.org/10.1080/05384680.1958.11904091.

Vader, A., 2022a. Chlorophyll A and phaeopigments Nansen Legacy cruise 2021704. University Centre in Svalbard. https://doi.org/10.21335/NMDC-966499899.

Vader, A., 2022b. Chlorophyll A and phaeopigments Nansen Legacy cruise 2019706. University Centre in Svalbard. https://doi.org/10.21335/NMDC-1109067467.

Vader, A., 2022c. Chlorophyll A and phaeopigments Nansen Legacy cruise 2019711. University Centre in Svalbard. https://doi.org/10.21335/NMDC-226850212.

Vader, A., 2022d. Chlorophyll A and phaeopigments Nansen Legacy cruise 2021703. University Centre in Svalbard. https://doi.org/10.21335/NMDC-983908955.

von Appen, W.-J., Waite, A.M., Bergmann, M., Bienhold, C., Boebel, O., Bracher, A., Cisewski, B., Hagemann, J., Hoppema, M., Iversen, M.H., Konrad, C., Krumpen, T., Lochthofen, N., Metfies, K., Niehoff, B., Nöthig, E.-M., Purser, A., Salter, I., Schaber, M., Scholz, D., Soltwedel, T., Torres-Valdes, S., Wekerle, C., Wenzhöfer, F., Wietz, M., Boetius, A., 2021. Sea-ice derived meltwater stratification slows the biological carbon pump: results from continuous observations. Nat. Commun. 12, 7309. https://doi.org/10.1038/s41467-021-26943-z.

Walker, E.Z., Wiedmann, I., Nikolopoulos, A., Skarðhamar, J., Jones, E.M., Renner, A.H. H., 2022. Pelagic Ecosystem Dynamics between Late Autumn and the Post Spring Bloom in a Sub-Arctic Fjord. Elem. Sci. Anth. 10 https://doi.org/10.1525/elementa.2021.00070.

Wassmann, P., 1998. Retention versus export food chains: processes controlling sinking loss from marine pelagic systems. In: Tamminen, T., Kuosa, H. (Eds.), Eutrophication in Planktonic Ecosystems: Food Web Dynamics and Elemental Cycling. Springer Netherlands, Dordrecht, pp. 29–57. https://doi.org/10.1007/978-94-017-1493-8_3.

Wassmann, P., Olli, K., Riser, C.W., Svensen, C., 2003. Ecosystem function, biodiversity and vertical Ffux regulation in the twilight zone. In: Wefer, G., Lamy, F., Mantoura, F. (Eds.), Marine Science Frontiers for Europe. Springer Berlin Heidelberg, Berlin, Heidelberg, pp. 279–287. https://doi.org/10.1007/978-3-642-55862-7_19.

Wassmann, P., Reigstad, M., Haug, T., Rudels, B., Carroll, M.L., Hop, H., Gabrielsen, G. W., Falk-Petersen, S., Denisenko, S.G., Arashkevich, E., 2006. Food webs and carbon flux in the Barents Sea. Prog. Oceanogr. 71.

Wassmann, P., Reigstad, M., 2011. Future Arctic Ocean Seasonal Ice Zones and implications for pelagic-benthic coupling. Oceanogr. 24 https://doi.org/10.5670/oceanog.2011.74.

Wassmann P., 2018. At the Edge- Current Knowledge from the Northernmost European Rim, Facing the Vast Expanse of the Hitherto Ice-Covered Arctic Ocean. Stamsund: Orkana.

Wessel, P., Smith, W.H.F., 1996. A global, self-consistent, hierarchical, high-resolution shoreline database. J. Geophys. Res. Solid Earth 101. https://doi.org/10.1029/96JB00104.

Wexels Riser, C., Reigstad, M., Wassmann, P., Arashkevich, E., Falk-Petersen, S., 2007. Export or retention? Copepod abundance, faecal pellet production and vertical flux in the marginal ice zone through snap shots from the northern Barents Sea. Polar Biol. 30 https://doi.org/10.1007/s00300-006-0229-z.

Wexels Riser, C., Wassmann, P., Reigstad, M., Seuthe, L., 2008. Vertical flux regulation by zooplankton in the northern Barents Sea during Arctic spring. Deep Sea Res. Part II 55. https://doi.org/10.1016/j.dsr2.2008.05.006.

Wiedmann, I., Reigstad, M., Sundfjord, A., Basedow, S., 2014. Potential drivers of sinking particle's size spectra and vertical flux of particulate organic carbon (POC): Turbulence, phytoplankton, and zooplankton. J. Geophys. Res. Oceans 119. https://doi.org/10.1002/2013JC009754.

Wiedmann, I., Reigstad, M., Marquardt, M., Vader, A., Gabrielsen, T.M., 2016. Seasonality of vertical flux and sinking particle characteristics in an ice-free high arctic fjord—different from subarctic fjords? J. Mar. Syst. 154 https://doi.org/10.1016/j.jmarsys.2015.10.003.

Wohlers, J., Engel, A., Zöllner, E., Breithaupt, P., Jürgens, K., Hoppe, H.-G., Sommer, U., Riebesell, U., 2009. Changes in biogenic carbon flow in response to sea surface warming. Proc. Natl. Acad. Sci. USA 106. Proc. Natl. Acad. Sci. https://doi.org/10.1073/pnas.0812743106.

Wold, A., Hop, H., Svensen, C., Søreide, J., Assmann, K.M., Ormancyk, M., Kwasniewski, S., 2023. Atlantification influences zooplankton communities seasonally in the northern Barents Sea and Arctic Ocean. Prog. Oceanogr. (Journal Preprint). https://doi.org/10.1016/j.pocean.2023.103133.